JOURNAL OF COMPUTATIONAL PHYSICS **136,** 559–579 (1997)
ARTICLE NO. CP975781

Stochastic Simulations of Two-Dimensional Composite Packings[1]

A. Albrecht,[2] S. K. Cheung, K. S. Leung, and C. K. Wong[3]

Department of Computer Science and Engineering, The Chinese University of Hong Kong, Sha Tin, N.T., Hong Kong

Received June 27, 1996; revised February 19, 1997

In recent years, dense packings of two- and three-dimensional objects have been studied intensely in the context of computational physics and material sciences. For example, computer simulations of disordered solids usually employ a two-dimensional model which is based on hexagonal networks of elastic and rigid bonds or arrangements of mixed soft and hard disks, respectively. Both types of bonds/disks are distributed randomly. Large systems of equations have to be solved at any simulation step for the calculation of local displacements or particle velocities. The simulations start from equidistant nodes of the hexagonal network or centers of disks, respectively, which, in general, may not be in an equilibrium state. We suggest an extension of the model where first a near-equilibrium packing of randomly distributed bonds/disks is calculated. Then, we can compute the displacement caused by external forces from this near-equilibrium initial packing of the elementary units. To this end, we propose a stochastic simulation of the external impact by incorporating the computation of near-equilibrium states as well as specific boundary conditions. Our methodology is based on a two-step approach consisting of a preprocessing stage, where physical properties of different types of particles are analyzed by numerical methods, and a second stage of stochastic (annealing-based) simulations which exploits approximate formulas for local interactions. We have implemented two types of cooling schedules with an expected serial run-time $n \cdot \ln^2 n$ and $n^{3/2} \cdot \ln^{5/2} n$, respectively, to reach near-equilibrium states for n disks. The algorithms were parallelized on a 20-processor machine, and for a sufficiently large number of objects the speedup is close to the number of processors. For example, the parallel run-time for computing near-equilibrium states is about $2\frac{1}{2}$ h for 449 disks, using the first cooling schedule, and about 37 h for 1068 disks, using the second cooling schedule. We performed a number of computer simulations calculating the average displacement in near-equilibrium states from regular, equidistant initial packings. The underlying physical model for our implementations is very similar to the model used for the analysis of granular composites which involves arrangements of mixed soft and hard disks. However, our emphasis is on the computational aspects rather than on particular systems of physical interactions, because substituting a system of physical interactions by another one does not affect significantly the run-time or the overall approach.

1. INTRODUCTION

Physical properties of composite materials have been studied recently by using discrete computational models related to packings of equal-sized disks in the plane. The approach is closely related to theoretical and numerical studies on two-dimensional random networks of rigid and nonrigid bonds. The basic methodology of the work dealing with random rigid–nonrigid networks comes from percolation theory [33]. An important parameter in percolation theory is the percolation threshold p_c, defining whether or not arbitrarily large clusters affected by percolation may appear. Obviously, p_c depends on the underlying network that represents the connection of elementary cells of the medium. In some cases, p_c can be calculated exactly, e.g., for hexagonal interconnections, where $p_c = 1 - 2 \cdot \sin(\pi/18)$. Networks representing elastic, granular materials are studied in particular for a fraction of rigid bonds that is close to the corresponding value of p_c. In a series of papers (see, e.g., [4–7, 10–13, 17, 25, 29, 31, 37]), material parameters like Poisson's ratio and related elastic moduli are analyzed theoretically and by numerical simulations for networks of randomly distributed rigid and nonrigid bonds, where the fraction p of rigid bonds satisfies $p \to p_c$ for $p < p_c$ and $p > p_c$. In most cases, the underlying network structure is hexagonal-like, and elementary bond-stretching and angle-bending force constants are assigned to the particular links. These constants differ significantly for rigid and nonrigid bonds, respectively. However, the distances between the nodes are assumed to be the same at the initial stage, despite the different values of assigned bond-stretching forces. Usually, the network has a variable length L_x and an elementary constant height L_y, and the external forces applied to nodes at one side are related to the relative displacement of network nodes by linear equations, according to the (hexagonal) network structure. In some applications, the rectangular $L_x \times L_y$ structure is replicated in the vertical direction with periodic boundary conditions [17]. Thus, by solving systems of linear equations, relative displacements can be calculated, keeping the balance to applied external forces; i.e., an equilibrium state of the system is reached by the displacements. The relation

[1] Research partially supported by the Strategic Research Program at The Chinese University of Hong Kong under Grant SRP 9505.

[2] On leave from BerCom GmbH, Bruno-Taut-Str. 4-6, D-12527 Berlin, Germany.

[3] On leave from IBM T. J. Watson Research Center, P.O. Box 218, Yorktown Heights, N.Y. E-mail: wongck@cse.cuhk.edu.hk.

0021-9991/97 $25.00

of displacements to applied forces from the boundary (e.g., perpendicular force, shear force) defines the corresponding elastic modulus. Due to the restricted height, the computation time is mainly defined by the length L_x.

Similar force/displacement relationships are considered for arrangements of rigid and flexible disks [5–7, 9, 20, 22] and for dense packings of spheres [38, 39]. In [20], for example, the packing of disks restrained by frictionless walls on three sides is considered, where a uniform velocity boundary condition is applied on the fourth side. If v_l denotes the velocity of unit u_l, the forces associated with a particular disk u_j are calculated from a contact scheme which is based on the forces $F_j(u_i) := \mu \cdot ((v_j - v_i)/R(u_i, u_j) - s)$; throughout this paper, ":=" means "is defined as." Here, μ is the contact viscosity relating the force and strain rate along the contact normal; $R(u_i, u_j)$ is the distance between the centers of u_i and u_j; and s denotes the sintering rate. The local relations are unified to a system of equilibrium equations which is solved with respect to the unknown velocities, e.g., for up to $n = 900$ units. These are then used to update the coordinates of the packing. As in the case of hexagonal networks, the initial packing is virtually assumed to be in an equilibrium packing of equidistant disks. This assumption is justified if relatively rigid components are considered for both types of disks and displacements are mainly caused by the external impact. But in [20], for example, the ratio of contact viscosities of the hard and soft particles is 10^{12}, and in [17] the ratio of rigid and nonrigid bond-stretching force constants is 10^7. In the case of such extreme differences between the viscosities in the equilibrium state one can expect significant displacements of particle positions from the regular, equidistant arrangement.

Our approach aims at the computation of equilibrium packing for a given number of disks within some rigid, in general irregular-shaped, boundary. The disks are of equal size but divided into two classes defined by the coefficient of elasticity. It is assumed that these coefficients differ significantly, and therefore, we distinguish between *rigid* and *flexible* disks. The elements of both classes are distributed randomly on the initial placement. Starting from a regular, hexagonal placement, the average displacement can be calculated after achieving a near-equilibrium packing of disks. For example, in the case of $n = 1068$ mixed rigid and flexible disks the average displacement in a near-equilibrium state compared to the equidistant initial placement is about 2% of the disk radius for a ratio 10^5 of force constants and very small initial deformations. Furthermore, the presence of an external impact will be modeled by initial intersections of disks with the boundary, where the force associated with the intersections is treated in a special way, different from contacts between disks. The displacements caused by the external impact are calculated from the near-equlibrium packing of disks.

From the viewpoint of computational complexity, an exponential time complexity can be expected for the calculation of displacements from external forces. To see why, we can look at the classical problem of packing and placing 2D objects, studied intensely in the past, for example, in the context of the 2D bin-packing problem [16, 18] and the placement of circuits on VLSI chips [30, 32, 36]. In these cases the objects are all assumed to be rigid, yet these problems have been proved to be computationally hard (NP-complete problems). Now, in the present case, we need to compute equilibrium states for packings of mixed rigid and flexible objects, which will add a new dimension to the computational task, because changing the position of a single disk by only a small value may cause changes in the positions of all other disks. As a consequence, we have to consider near-equilibrium states as approximate solutions to the original problem.

In deterministic approaches, the near-equilibrium states and, therefore, the relative displacements, are calculated by an iterative process, where at any single step polynomial time matrix operations (computing solutions for systems of linear equations) are applied. These polynomial time operations are repeated a large number of steps until some stopping criterion is satisfied, i.e., an approximate solution has been calculated. For example, in [5] the iterations are continued until the changes of calculated relative displacements are smaller than 10^{-5}.

Our methodology is based on a two-step approach consisting of a preprocessing stage, where deformation/force relationships of particles are analyzed separately for each homogeneous material of particles by proven numerical methods. The application of numerical methods is based on known material coefficients at the particle level. At the second stage, (near-)equilibrium configurations of the entire system of n particles are computed by stochastic simulations, in order to obtain information about physical properties of the composite material. At this stage, approximations of local interactions of particles are employed which have been derived at the first stage. The technique of simulated annealing, in particular, seems to be an appropriate stochastic method for computing near-equilibrium states of dense packings, since annealing-based optimization algorithms originated from Metropolis' method [26] of computing equations of state for substances consisting of interacting individual molecules. In [39] (see Section 2.4 there), the computation of equlibrium configurations of nontouching spheres is performed at the initial stage of calculating densifications of spheres. The procedure is based on Metropolis' method; however, it is not mentioned explicitly whether the running time of the preprocessing step was included in the run-time analysis provided in [39]. But in Section 3 of [39], the need for fast algorithms producing initial equilibrium states is emphasized (see the reference to [21] there).

In general, simulated annealing algorithms are relatively slow, but in our specific case we can employ a special type of objective function and take advantage of the structure of the underlying configuration space, namely, although the position and shape of a single object has an impact on all other elements of the system, to change from one configuration to another involves only local computations. This is an important difference from other applications of simulated annealing algorithms, e.g., in the area of VLSI design (see [30, 32, 36]).

Based on the general framework of simulated annealing, we have designed two specifically tailored heuristic procedures computing equilibrium placements of mixed rigid and flexible objects. For the expected run-time of these heuristics the upper bounds $n \cdot \ln^2 n \cdot \overline{\chi}$ and $n^{3/2} \cdot \ln^{5/2} n \cdot \overline{\chi}$, respectively, can be proved, where $\overline{\chi}$ denotes the average value of the expected ratio of all trials to the number of accepted moves, taken over all values of the cooling parameter, and n is the number of placed objects (an outline of the proofs will be given in Section 4). The objective function represents the average value of local forces ''trying to move'' the particular units. A randomly chosen disk is moved a single grid step (which is significantly smaller than the diameter of disks) in a randomly chosen direction. All other disks remain unchanged. The changes of local forces (velocities) have to be calculated only for the moved unit and the neighbouring units that are affected by the move (as in other papers on simulations of disordered materials, see [5, 6, 17, 20]). Therefore, the ''updating'' of physical values of a single unit after a single computational step has to be performed only with respect to a constant, local neighborhood, which is independent of the variable (and large) number n of all units of the system. In other words, the overall run-time depends only by a constant factor on the particular system of local physical interactions. We obtain a further speedup of the computation, i.e., a decrease of the constant factor, by introducing an approximate formula which represents the deformation/force relationship between neighboring disks. The approximate formula takes into account different types of contacts, e.g., contacts between flexible and rigid units. After the new value of the objective function has been calculated, a random decision rule related to the change of the objective function is applied, and the outcome defines whether or not the move will be accepted and indeed performed. Since the change of the objective function can be calculated very efficiently from the previous value, independent of the number of objects participating in the packing problem, the algorithms run relatively fast and depend mainly on the number of ''cooling steps'' and the length of Markov chains at a fixed ''temperature.''

In Section 2, we introduce our physical model, including the derivation of an approximate deformation/force relationship. Furthermore, we will discuss the relation to other models from the literature we already referred to. The deformation/force relationship is derived from numerical experiments which are based on the finite element method and performed on several materials. Since an approximate formula is used for the physical modeling, instead of the time-consuming finite element method, the computation of local forces resulting from deformations can be performed relatively fast, i.e., in constant time related to the grid size, the material constants, and the diameter of units, but independent of the number of placed units. Throughout the paper we will emphasize the complexity aspects of computing equlibrium states of mixed rigid and flexible objects, demonstrated on the particular physical model introduced in Section 2. The computation of equilibrium states is explicitly discussed in [5, 6, 31, 39]. The underlying algorithm from [31, 39] is Metropolis' method. In [5, 6], near-equilibrium states are calculated from linear systems of equations, solved on Cray X-MP/Y-MP machines. In Section 3, we describe the general structure of simulated annealing algorithms, and in Section 4, our stochastic annealing procedures, calculating equilibrium packings of mixed rigid and flexible objects, are explained in more detail. Experimental results are presented in Section 5, including the outcome of parallel implementations on a 20-processor Sun SPARC2000 machine. The implementations are running under OS Solaris 2.4 for both the single-processor and parallel modes. The computational experiments were performed for both types of cooling schedules and for up to 1500 disks, where the fraction of rigid disks is close to the percolation threshold $1 - 2 \cdot \sin(\pi/18)$.

2. PHYSICAL MODEL

2.1. *Basic Notations*

We consider the placement of flexible disks within a rigid rectangular boundary. The disks are of equal size with diameter d and built from at most two different types of materials. By L and H we denote the length and the height of the boundary, respectively. For the $L \times H$ placement region a subdivision by a grid of step size w is performed in both directions, and it is assumed that L and H are both multiples of the elementary grid unit w. We denote $h := h_w := H/w$ and $l := l_w := L/w$. The center Z of a single unit can be placed only into one of the $K := (h - 1) \cdot (l - 1)$ grid nodes, excluding the nodes on the boundary. It is assumed that the lower left corner of the rectangular boundary is the origin of the coordinate system which is defined by the unit measured in w.

If two disks intersect, this intersection is interpreted for both disks as a *deformation* of depth Δ. The value Δ is the distance measured on the line connecting the centers from the intersecting point on the original border (the arc) to the chord halving the distance between the centers (see

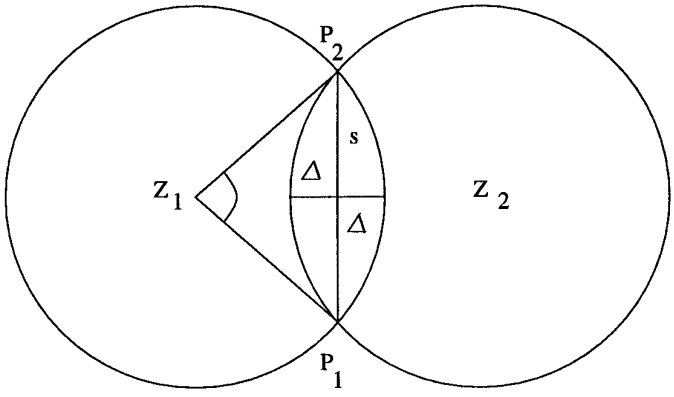

FIGURE 1

Fig. 1). The length of the chord between the two points P_1 and P_2, where the borders cross, is denoted by s and called the *deformation length*. The relationship between the deformation depth and the deformation length is expressed by the formula

$$s = 2 \cdot \sqrt{\Delta \cdot d - \Delta^2}.$$

The angle defined by P_1, Z_1, and P_2 is called the *deformation angle* and can be calculated by

$$\alpha = 2 \cdot \arcsin\left(2 \cdot \sqrt{\frac{\Delta}{d} - \left(\frac{\Delta}{d}\right)^2}\right).$$

By $R = R(Z_1, Z_2)$ we denote the distance between the centers of disks. In our model we assume that the maximum deformations of a disk are bounded by the limit of elasticity of the material. Let $D_{\max}$ denote this upper bound for deformations, which is a constant depending on the material and the size of disks. For any placements, one has to ensure that the limit of elasticity is not violated, i.e., the centers of the disks have to be separated by a distance of at least $R \geq d - 2 \cdot D_{\max}$. Given a placement P, one can calculate for any unit u the maximum deformation $\Delta(u)$ resulting from "intersections" with other disks. By $\Delta_{\max} := \max_u \Delta(u)$ we denote the maximum deformation that a single unit is exposed in P. Hence, in a physical feasible placement P we have $\Delta_{\max} \leq D_{\max}$.

With any deformation Δ of the disk u we associate a force $\mathbf{F}(u, \Delta)$, calculated from the "intersection" of disks :

$$\mathbf{F}(u, \Delta) := \frac{1}{s} \cdot \int_{s(\Delta)} \mathbf{f}\, dx,$$

where $\mathbf{f}(x)$ is the force at point x of the chord $\overline{P_1 P_2}$ (see Fig. 1), trying to recover the original shape of u. The force $\mathbf{F}(u, \Delta)$ is associated with a single deformation Δ of a given disk u. This force is acting on the neighboring disk as well as on the disk u itself. As a result, the vector sum of all acting forces is equal to zero, and for a particular disk u and a particular deformation Δ we have to take into account the force $\mathbf{F}(u', \Delta)$ from the neighboring unit u' and the force $\mathbf{F}(u, \Delta)$, which are both oriented into the same direction. Therefore, in the case of only a single material of objects, the forces are easily calculated by doubling the force associated with a single deformation. For placements of mixed rigid and flexible objects, one has to calculate each force individually for the particular material. In Fig. 2, e.g., $\mathbf{F}_1$ represents the sum of the forces which are calculated for both materials participating in the corresponding deformation. Thus, if a disk u intersects with several other disks or parts of the boundary, one has to compute the forces $\mathbf{F}_i = \mathbf{F}(u, \Delta_i) + \mathbf{F}(u_i, \Delta_i)$ for each Δ_i. Then, the resultant force $\mathbf{F}_{\text{res}}(u) = \Sigma_i\, \mathbf{F}_i$ is calculated from the vector sum, where the origin of $\mathbf{F}_{\text{res}}(u)$ is supposed to be the center of the disk (see Fig. 2). From the viewpoint of a particular disk, the resultant force $\mathbf{F}_{\text{res}}(u)$ tries to move the disk u into its direction. The particular forces $\mathbf{F}(u, \Delta)$ are calculated from an approximate force/deformation relationship, which will be derived in Section 2.2. If for all disks $\mathbf{F}_{\text{res}}(u) < \varepsilon$ for a small ε, the packing is said to represent a (near-)equilibrium state.

Similar relationships are used, e.g., in [5, 6, 20] for the description of local interactions. In [5–7], vector transport and failure properties of disordered materials are studied. The underlying model is a percolation network in which each bond represents an elastic element, or a spring, with an elastic constant η which can take on values from a

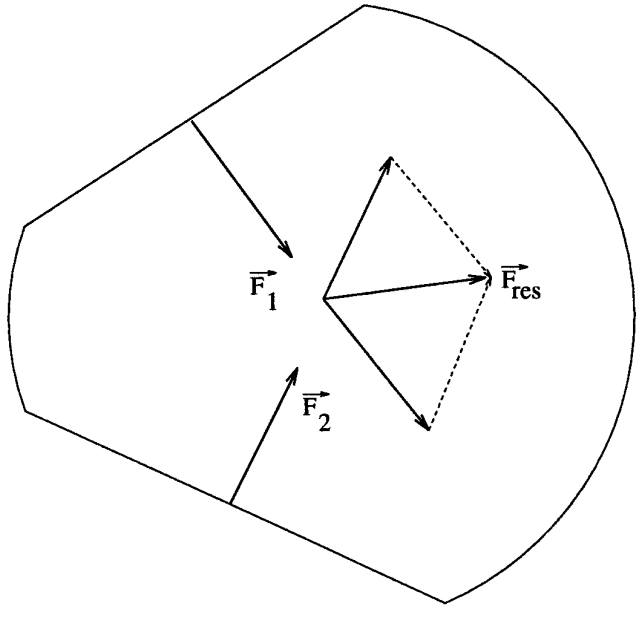

FIGURE 2

probability distribution (in most cases η takes the value a and b with probability p and $1 - p$, respectively). The basic relation is given by the elastic energy $\mathbf{E}$ of a percolation network which is defined as

$$\mathbf{E} = \frac{1}{2} \cdot \sum_{\langle ij \rangle} [(\mathbf{u}_i - \mathbf{u}_j) \cdot \mathbf{F}_{ij}]^2 \cdot \eta_{ij}.$$

Here, $\mathbf{u}_i$ denotes the displacement of the ith node, $\mathbf{F}_{ij}$ is the force acting between nodes, and η_{ij} stands for the corresponding elastic constant. To calculate elastic properties, the elastic energy $\mathbf{E}$ has to be minimized with respect to $\mathbf{u}_i$; i.e., $\partial \mathbf{E}/\partial \mathbf{u}_i = 0$. This condition, written for any node i, leads to a system of linear equations. The boundary conditions depend on the modulus that has to be calculated. From a numerical solution of the system new coordinates can be calculated, and the procedure is repeated k steps until $|\mathbf{u}_i^{(k+1)} - \mathbf{u}_i^{(k)}|/|\mathbf{u}_i^{(k)}| < \varepsilon$ is satisfied for any node i, where, e.g., $\varepsilon = 10^{-5}$. The computations presented in [5, 6] were performed on Cray X-MP/Y-MP machines.

The force/velocity relationship $F_j(u_i) := \mu \cdot (v_j - v_i)/R(u_i, u_j) - s)$, which is employed in [20] within the *truss* model, was already mentioned in Section 1. The forces $F_j(u_i)$ are used only for the formulation of equilibrium conditions; i.e., the essential values are the "velocities" v_i. In fact, this formula takes into account an increase of the force depending on the deformation, which is expressed by the inverse value $R^{-1}(u_i, u_j)$ of the distance. Properties of the material (contact viscosity) are included by the coefficient μ. The parameter $-s$ is related to the specific problem of sintering rates in granular composites; in particular, the sintering problem is converted into a problem for the deformation of disks to certain forces. The equilibrium equations for all particles in the packing are assembled into a linear system which is solved for the unknown velocities v_i. These are then used to update the coordinates of the packing; i.e., the approach is similar to the method described in [5, 6] and, e.g., in [17]. Basically, the underlying force/deformation relationship employed in this model is proportional to $\mu/R(u_i, u_j)$.

The calculation of elastic moduli is based on simulations of an external impact on the elastic material. In the deterministic approach, as performed in [5, 6, 17, 20], external forces are taken into account by the linear system of equilibrium equations. In our stochastic approach, we first calculate a near-equilibrium packing, starting from random or regular initial placements. Then, the existence of external forces, say, at the upper boundary, is modeled by lowering the upper boundary, i.e., the size of the packing area is decreased in one direction. Thus, only normal forces, perpendicular to the boundary, can be simulated. Furthermore, the depth of intersections is restricted by the radius of disks. Larger external forces have to be simulated stepwise. Future work will be directed on further extensions of the model, where, e.g., various (concave) shapes of the boundary will be considered.

2.2. *Deformations of Elastic Materials*

In the literature on material sciences, in particular on flexible materials (see, e.g., [35]), the relationship between deformations and forces is expressed as a closed-form formula only for small values of deformations, i.e., small displacements of points relative to adjacent points. Therefore, the calculation of the force related to a given deformation and vice versa is performed for infinitesimal elements of an object. Large scale deformations have to be calculated by time-consuming numerical methods. In our case of granular composites, we have to deal with relatively large particles, where significant deformations cannot be excluded. For example, the size of objects considered in [4] for experimental studies on elastic percolation networks represents the order of magnitude of 1 mm (however, this is supposed to be an upper bound), and the forces associated with displacements are ranging from 0.2 N to 10 N. Thus, we try to derive an approximate force/deformation relationship which avoids time-expensive numerical calculations.

Commonly, the notion *force* is used for an external impact related to an object, while the notion *stress* refers to internal forces acting on infinitesimal elements of an object. Thus, given an infinitesimal cubic element whose edges are parallel to the coordinate axes x, y, and z, we consider the stress vectors $\mathbf{F}_x$, $\mathbf{F}_y$, and $\mathbf{F}_z$ acting on the cube faces. For example, the stress $\mathbf{F}_x$ is related to the yz plane. In our problem setting, these stress vectors are interpreted to be the result of deformations; i.e., these forces try to re-establish the original point positions of the cube. The stress vectors are resolved into their components, e.g., $\mathbf{F}_x$ into σ_{xx}, σ_{xy}, and σ_{xz}. The components of the stress vector $(\mathbf{F}_x, \mathbf{F}_y, \mathbf{F}_z)$ are considered in their relation to the *relative* displacement of points within the cubic element. Therefore, given a displacement of a point (x, y, z) to the position $(x + u, y + v, z + w)$, we additionally consider the *relative* displacement of the two adjacent points (x, y, z) and $(x + dx, y + dy, z + dz)$. The partial derivatives $\partial u/\partial x$, $\partial u/\partial y$, ..., etc. represent the strength of the relative displacement along the x-axis, y-axis, and z-axis, respectively. These partial derivatives are called the physical *strain* defined by the relative displacement of points. For example, $e_{xx} := \partial u/\partial x$ is the physical strain along the x axis (the index xx results from the displacement u along the x-axis and the partial derivative in the x direction). In the theory of elasticity, the following formula is used for the relationship between stress and strain, where we consider only the case of e_{xx} along the x-axis and the components of stress σ_{xx}, σ_{yy}, and σ_{zz}:

$$e_{xx} = \frac{1}{E} \cdot \sigma_{xx} - \frac{\nu}{E} \cdot (\sigma_{yy} + \sigma_{zz}). \tag{1}$$

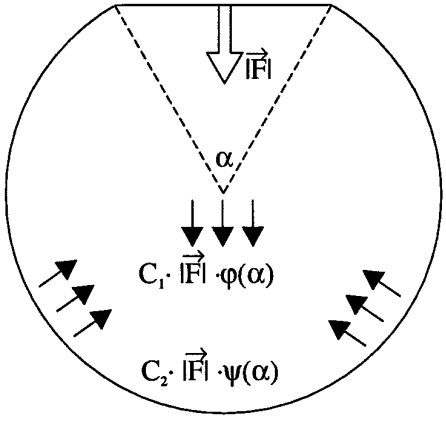

FIGURE 3

The values σ_{yy} and σ_{zz} are derived from the stress acting on the zx plane and xy plane, respectively. The constant E denotes Young's modulus and ν is the notation for Poisson's ratio. Similar relationships are used in the theory of elasticity for the three quantities of shear strain, e.g., $e_{xz} = (1/G)\ \sigma_{xz}$, where $G = \mathrm{E}/2 \cdot (1 + \nu)$ is the torsional or shear modulus.

Since we consider the two-dimensional case, we can set $\sigma_{zz} = 0$, and (1) becomes

$$e_{xx} = \frac{1}{E} \cdot \sigma_{xx} - \frac{\nu}{E} \cdot \sigma_{yy}. \tag{2}$$

As the partial derivative $\partial u/\partial x$, the value e_{xx} measures changing lengths, while σ_{xx} and σ_{yy} are components of stress vectors. That means, (2) describes a relation between relative displacements and related forces. Based on (2), one could suggest the formula $\Delta = (1/E)\ F - (\nu/E)\ F'$ to be taken as the deformation/force relationship in the case of a single, relatively large deformation. However, as can be seen from numerical experiments, this formula does not match the force values F computed for a number of different deformations Δ. The experiments were performed on several flexible materials by using finite element methods with relatively dense meshes (see Section 2.3). Following the general structure of (2), the search range for an approximate formula, expressing the relation between a *single* deformation and the resulting force, was restricted to the type

$$\Delta = C_1 \cdot |\mathbf{F}| \cdot \varphi(\alpha) - C_2 \cdot |\mathbf{F}| \cdot \psi(\alpha), \tag{3}$$

where C_1, C_2 are constants, α denotes the deformation angle, and $\mathbf{F}$ is the force, acting through the center of the deformation (see Fig. 3). The first term in this formula represents the deformation that would appear "without resistance" from all parts of the object, the second term stands for the decrease of deformation that is caused by the internal resistance of the material, e.g., caused by the deformation of the boundary in the opposite direction (see Fig. 3). In the case of more than a single deformation, the force associated with a particular deformation will be calculated in the same way as given in formula (3).

The function $\varphi(\alpha)$ should ensure $|\mathbf{F}| = 0$ for $\Delta = 0$. For simplicity and because of C_1, we require $\varphi(0) = 1$. Formally, we take into account extremely large deformations, i.e., Δ is upper bounded by $d/2$, and for very large Δ the force should increase rapidly. Therefore, additionally,

$$\varphi(\alpha_1) > \varphi(\alpha_2) \quad \text{for } \alpha_1 < \alpha_2 \leq \pi$$

is required. For the second function we set $\psi(0) = 0$, i.e., the internal resistance is equal to zero if no deformation occurs. With an increasing deformation, the internal resistance also increases:

$$\psi(\alpha_1) < \psi(\alpha_2), \quad \text{where } \alpha_1 < \alpha_2 \leq \pi. \tag{4}$$

Numerical experiments for deformation angles up to $\pi/2$ have shown that $\varphi(\alpha)$ can be approximated by $1/(1 + \xi(\alpha))$, where $\xi(\alpha)$ is a slowly growing function, e.g., $\xi(\alpha) = \ln(1 + \alpha/2)$ or $\xi(\alpha) = \sin(\alpha/2)$. However, in this case one can use the expansion

$$\frac{1}{1 + \xi(\alpha)} = 1 + \sum_{n=1}^{\infty} (-1)^n \cdot \xi^n(\alpha)$$

and take only the first terms of this representation. Applying this approximation, (3) becomes

$$\begin{aligned} \Delta &= C_1 \cdot |\mathbf{F}| \cdot \left(1 + \sum_{n=1}^{\infty} (-1)^n \cdot \xi^n(\alpha)\right) - C_2 \cdot |\mathbf{F}| \cdot \psi(\alpha) \\ &\approx C_1 \cdot |\mathbf{F}| \cdot (1 - \xi(\alpha)) - C_2 \cdot |\mathbf{F}| \cdot \psi(\alpha) \\ &= C_1 \cdot |\mathbf{F}| - (C_1 \cdot \xi(\alpha) + C_2 \cdot \psi(\alpha)) \cdot |\mathbf{F}|. \end{aligned}$$

But this relation means that a priori the search range can be restricted to

$$\Delta = C_1 \cdot |\mathbf{F}| - C_2 \cdot |\mathbf{F}| \cdot \zeta(\alpha),$$

where $\zeta(\alpha) := (C_1/C_2)\ \xi(\alpha) + \psi(\alpha)$ satisfies (4), because $\xi(\alpha)$ and $\psi(\alpha)$ are increasing functions. Approximations for $\zeta(\alpha)$ and the constants C_1 and C_2 are derived from numerical experiments (see Section 2.3).

As a result of the data analysis, the following formula is assumed to reflect approximately the relationship between

the deformation Δ and the resulting force $\mathbf{F}$ for a relatively large range of deformations:

$$\Delta = C_1 \cdot |\mathbf{F}| - C_2 \cdot |\mathbf{F}| \cdot \left(\frac{\alpha}{2} + \sin\frac{\alpha}{2}\right). \tag{5}$$

The ratio $\alpha/2$ was chosen in order to ensure monotonicity also for large values $\alpha \leq \pi$, and we assume that $C_1 - C_2 \cdot (\pi/2 + 1) > 0$ is satisfied. The monotonicity is desirable in order to enhance the performance of our stochastic algorithms: In simulations of disordered materials, usually a number of simulations are performed for randomly generated (regular) initial configurations (distributions of rigid/nonrigid disks or bonds). In the case of the disk model, the relative positions of rigid/nonrigid disks in randomly generated configurations might be far from the positions in equilibrium configurations (i.e., it could be necessary that particular disks ''walk'' around relative large distances, comparable to the disk diameter). If only very small deformations are allowed, randomly generated configurations which are ''close'' to equilibrium configurations (i.e., where ''long walks'' are not necessary) might appear only in a long chain of random generations. The other way is to allow large deformations (which are physically not feasible, but appear only in initial and intermediate configurations, and usually disappear in the final result close to an equilibrium state), which make it ''easy to walk'' relative long distances for particular disks in order to find equilibrium configurations. Therefore, in this case a single random configuration covers a (large) number of random trials.

If Δ is replaced by $(d/2)\ (1 - \cos(\alpha/2))$, one obtains

$$|\mathbf{F}| = \frac{d}{2} \cdot \frac{1 - \cos(\alpha/2)}{C_1 - C_2 \cdot (\alpha/2 + \sin(\alpha/2))}. \tag{6}$$

The force $\mathbf{F}$ represents $\mathbf{F}(u, \Delta)$ defined in Section 2.1. This force is acting at the center of the deformation, where the deformation depth is equal to Δ. If a single unit is ''intersecting'' with several other units, the intersection line, in general, is not equal to $s(\Delta)$ (see Fig. 4). But $\mathbf{F}$ was taken to represent the forces $\mathbf{f}(x)$ from the entire deformation length $s(\Delta)$. In order to take into account only the actual force associated with the length $l(u, v)$ of the intersection line between two units (see Fig. 4), the following modification of formula (6) is introduced: The force $\mathbf{F}$ is divided by the deformation length $s(\Delta)$ and then multiplied by $l(u, v)$:

$$|\mathbf{F}_{\text{norm}}| = \frac{l(u, v)}{C_1 - C_2 \cdot (\alpha/2 + \sin(\alpha/2))} \cdot \frac{\Delta}{s(\Delta)}. \tag{7}$$

Since we employ in the following only (7), we will use, in general, the notation $\mathbf{F}$ instead of $\mathbf{F}_{\text{norm}}$.

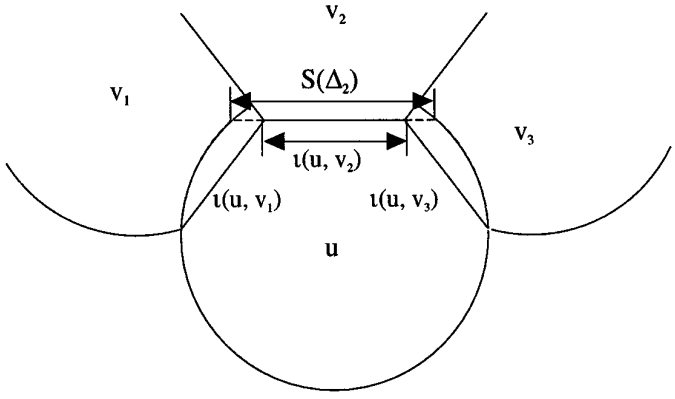

FIGURE 4

That the force in (5) increases monotonically with α, i.e., that the first derivative is positive on $\alpha \in (0, \pi)$, follows from our construction of formula (5). By straightforward calculations one can show that the second derivative $d^2F/d\alpha^2$ is also positive for $\alpha \in (0, \pi)$. This is important for our simulated annealing procedures (see Section 4.1).

We use the notation *rigid* disk for materials where C_1 and C_2 from formula (7) are small constants ($\ll 10^{-5}$ mm/N; see Section 2.3).

Thus, our approach consists of the following steps: First, disks, i.e., particles of the same homogeneous material, are analyzed by numerical methods, based on known material constants like Poisson's ratio and Young's modulus. From this analysis, the necessary parameters of the approximate formula (7) are derived, which is designed to describe the deformation/force relationship at the particle level. Then, at the second step, elastic properties of composite packings are studied by stochastic simulations, where the approximate formula (7) is employed for the calculation of resultant forces assigned to particular disks.

2.3. *Numerical Experiments on Elastic Materials*

The relationship between deformations and forces was analyzed by a number of numerical experiments, performed on different flexible materials and sizes of particles, respectively. The experiments were based on the finite element method, implemented within the software package CADDS 5 that was used for the modeling of flexible disks. The diameter of disks was between 1 mm and 10 mm (see [4]), the thickness by one order of magnitude smaller than the diameter. The material constants, i.e., Poisson's ratio and Young's modulus were taken from [8, 35]. In general, the material constants are ranging within some limits, and the average value was taken as the input value.

Three different angles were considered in detail: $\alpha_1 = \pi/4$, $\alpha_2 = \pi/6$, and $\alpha_3 = \pi/12$. In most cases, the mesh of

TABLE I

Material	Density g/cm^3	C_1 mm/N	C_2 mm/N
Acrylics	1.18	1.14×10^{-4}	4.47×10^{-5}
Low-density polyethylenes	0.91	1.21×10^{-2}	4.69×10^{-3}
Medium density polyethylenes	0.93	7.54×10^{-3}	3.20×10^{-3}
High-density polyethylenes	0.95	2.46×10^{-3}	8.56×10^{-4}
Thermoplastic elastomer polyurethane	1.10	2.07×10^{-3}	7.42×10^{-4}

nodes for the finite element method was defined by 53 nodes on the circular boundary between P_1 and P_2 for $\alpha_1 = \pi/4$, and 11 nodes on P_1Z_1 and P_2Z_1 (see Fig. 1). Triangular-shaped finite elements were used for the analysis. The calculation of the unknowns C_1, C_2 was performed by using the three combinations of data: $[\pi/4, \pi/6]$, $[\pi/4, \pi/12]$, and $[\pi/6, \pi/12]$. The numerical results are from stable regions of experimental data, obtained by further experiments with different (in particular larger) numbers of nodes. For small angles it was possible to perform experiments with meshes of high density. The ratio **r** of deformation and force was growing with the density of meshes, e.g., for the deformation angle $\alpha = \pi/12$ from $\mathbf{r} = 0.00169$ mm/N (19 nodes between P_1 and P_2) up to $\mathbf{r} = 0.00187$ mm/N (27 nodes). But this is considered to be a small difference.

The values of the constants C_1 and C_2 given in Table I satisfy with one exception (medium density polyethylenes) the condition $C_1 - C_2 \cdot (\pi/2 + 1) > 0$ (see the conditions required for (7)). But in all five cases the absolute value $|C_1 - C_2 \cdot (\pi/2 + 1)|$ is significantly smaller, compared to C_2. The deviation for different sizes is up to 14%, the average deviation is 8%. Thus, if the size of the particles is known, one can define the constants C_1 and C_2 more specifically. We will apply the values from Table I in Section 5 to the sizes of particles ranging between 0.1 mm and 1 mm.

3. SIMULATED ANNEALING ALGORITHMS

Simulated annealing was introduced in [23] as a new approach to calculate approximate solutions of combinatorial optimization problems, where the underlying framework was based on Metropolis' method [26] of computing equilibrium states for substances consisting of interacting molecules. Detailed information about this method and applications in different areas can be found in [1, 2, 19, 23, 24, 27, 28, 32, 34, 36]. We will follow mainly the notations provided in [2, 24].

Simulated annealing algorithms are acting within a configuration space $\mathscr{C}_n$ in accordance with a certain neighbourhood structure $\mathscr{N}$, where the particular steps are controlled by the value of an objective function $\mathscr{Z}$. Now we are going to introduce these notions for placements of mixed flexible and rigid objects.

3.1. *Configuration Space and Neighbourhood Relation*

We suppose that the center of a single disk can be placed into K grid nodes, excluding the nodes on the boundary. We require that different disks be placed into different grid nodes. The corresponding set of placements is denoted by $\mathscr{C}_n$ and is called the *configuration space*. The size $|\mathscr{C}_n|$ of the configuration space can be upper bounded as follows, where we take into account the maximum allowable deformation $D_{\max}$ and the lower bound

$$A_{\min}(D_{\max}) \geq \frac{\pi}{4} \cdot (d - 2 \cdot - D_{\max})^2 \tag{8}$$

for the area of a deformed disk. For n disks, there are at most K possibilities to place the first unit. The ith disc can be placed into at most $K - (i-1) \cdot \lfloor A_{\min}/w^2 \rfloor$ grid nodes. Hence, the upper bound

$$|\mathscr{C}_n| < K^n \cdot \prod_{i=1}^{n} (1 - (i-1) \cdot \mathbf{a}) \tag{9}$$

$$< K^n \cdot \left(1 - \frac{n-1}{2} \cdot \mathbf{a}\right)^n, \tag{10}$$

is valid, where

$$\mathbf{a} := \frac{1}{K} \cdot \left\lfloor \frac{A_{\min}}{w^2} \right\rfloor.$$

Furthermore, we suppose $n \cdot (\pi/4) \cdot d^2 \geq h \cdot l \cdot w^2/c$, where c is a constant defined by the maximum number of disks that can be placed without deformations (the constant is approximately equal to 1.103). If the inequality is violated, the computation of equilibrium states becomes trivial, because the n units can be moved rapidly into a hexagonal-like position where no forces are acting on the unit. From this condition we obtain the relation:

$$n > K \cdot \frac{4 \cdot w^2}{c \cdot \pi \cdot d^2}. \tag{11}$$

Together with (10), the upper bound (11) illustrates the exponential relation between $|\mathscr{C}_n|$ and the number of units n. Furthermore, (10) is of special interest for the estimation of the running time (see Section 4.3).

The transitions between placements are defined as a subset $\mathcal{N}$ of the Cartesian product $\mathcal{C}_n \times \mathcal{C}_n$; i.e., it is not allowed to place more than one center of an object into a single grid node. The ordered pair $[P, P'] \in \mathcal{C}_n \times \mathcal{C}_n$ is included into $\mathcal{N}$, iff P and P' differ at most in the position of a single object and the center of this object is located in neighbouring grid nodes. Two nodes of the grid are considered to be neighbouring, if their coordinates differ only by one measure unit. For example, (x, y) and $(x - 1, y + 1)$ are neighbouring nodes. The definition of $\mathcal{N}$ includes $[P, P] \in \mathcal{N}$. Because a grid node, except the nodes on the boundary, has eight neighbours, the number of P' in pairs $[P, P'] \in \mathcal{N}$ is upper bounded by $8 \cdot n + 1$, if P consists of n units. The lower bound is $|\mathcal{N}| \geq 12 \cdot \lfloor \sqrt{n} \rfloor - 3$ for a dense square packing of all n objects.

3.2. *The Objective Function*

For each disk u_j, $j = 1, 2, ..., n$, we define the set $S(u_j)$ of surrounding disks that may cause a deformation of u_j. The set $S(u_j)$ can be calculated by searching in a distance smaller than d from the center of u_j, and the particular elements of $S(u_j)$ can be calculated in time $(d \cdot \log K)^{O(1)}$. Here we assume a binary representation length $\log x$ and a polynomial complexity of arithmetic operations with respect to $\log x$. Let m denote the number of forces $\mathbf{F}^{(i)}$ applied from different sides to u_j, $i = 1, 2, ..., m$ (see Fig. 2 for $m = 2$). We suppose that the forces $\mathbf{F}^{(i)}$ are ordered, e.g., counterclockwise with respect to their appearance at the border of u_j. If $R(u_i, u_j) < d$, i.e., $u_i \in S(u_j)$, the resulting deformation $\Delta_{ij} > 0$ is calculated by $\Delta_{ij} := \frac{1}{2} \cdot (d - R(u_i, u_j))$. Furthermore, the length $l(u_j, u_i)$ of the intersection line is calculated from the centers (x_i, y_i), (x_j, y_j), and the diameter d (see Fig. 4). With any pair $[\Delta_{ij}, l(u_i, u_j)]$, a force $\mathbf{F}^{(i)}$ is associated in accordance with the approximate formula (7). The forces $\mathbf{F}^{(i)}$ assigned to a unit are used for the calculation of the resultant force $F(u_j)$. In a similar way the interactions with the boundary are considered, where $\Delta_j := (d/2 - R(u_j))$ for a single intersection.

For the calculation of the resultant force $\mathbf{F}(u_j)$ we have to define the direction of the forces $\mathbf{F}^{(i)}$. This direction is determined by the counterclockwise angle α_{ij} between the x axis and the line connecting the centers of u_i and u_j. The force $\mathbf{F}(u_j)$, which "tries to move" u_j, is calculated recursively, building pairwise the vector sum of two forces. The complexity of these local computations depends on m and d, but for m we have

$$m \leq \frac{2 \cdot \pi}{2 \cdot \arcsin(1/2 - \Delta_{\max}/d)}.$$

Therefore, the complexity of calculating a particular resultant force $\mathbf{F}(u_j)$ $j = 1, ..., n$, including the direction of $\mathbf{F}(u_j)$, is upper bounded by $(d \cdot \log K)^{O(1)}$.

We introduce the following objective function:

$$\mathcal{Z}(P) := \frac{1}{n} \cdot \sum_{j=1}^{n} |\mathbf{F}(u_j)|, \tag{12}$$

where $P \in \mathcal{C}_n$.

DEFINITION 1. A placement P is said to be in an equilibrium state, iff $\mathcal{Z}(P) = 0$.

Because in our case the placements depend on a grid structure, it cannot be expected, in general, that there exist placements in an equilibrium state within $\mathcal{C}_n$. Therefore, we consider the minimization of $\mathcal{Z}(P)$ on the grid structure and define

$$\mathcal{C}_n^{\text{opt}} := \{Q : \forall P(P \in \mathcal{C}_n \rightarrow \mathcal{Z}(P) \geq \mathcal{Z}(Q))\}.$$

As already mentioned in Section 1, the complexity of computing elements of $\mathcal{C}_n^{\text{opt}}$ is expected to be exponentially in n. Thus, stochastic algorithms are considered for finding packings close to elements from $\mathcal{C}_n^{\text{opt}}$.

3.3. *General Structure of Simulated Annealing*

First, we have to define how the transitions between placements depend on the objective function $\mathcal{Z}$. Given a pair of placements $[P, P'] \in \mathcal{N}$, we denote by $G[P, P']$ the probability of generating P' from P and by $A[P, P']$ the probability of accepting P', once it has been generated from P. Since we consider a single step of transitions, the value of $G[P, P']$ depends on the set $\mathcal{N}_P := \{P' : [P, P'] \in \mathcal{N}\}$. In most cases, a uniform probability with respect to P is taken by setting

$$G[P, P'] := \begin{cases} \dfrac{1}{|\mathcal{N}_P|}, & \text{if } P' \in \mathcal{N}_P, \\ 0, & \text{otherwise.} \end{cases} \tag{13}$$

Based on the above-mentioned upper and lower bounds for $\mathcal{N}_P$, one obtains for n objects and $P' \in \mathcal{N}_P$,

$$\frac{1}{8 \cdot n + 1} \leq G[P, P'] \leq \frac{1}{12 \cdot \lfloor \sqrt{n} \rfloor - 3}. \tag{14}$$

As for $G[P, P']$ there are different possibilities for the choice of acceptance probabilities $A[P, P']$. A straightforward definition related to the underlying analogy to thermodynamical systems is

$$A[P, P'] := \begin{cases} 1, & \text{if } \mathcal{Z}(P') - \mathcal{Z}(P) \leq 0, \\ e^{-(\mathcal{Z}(P') - \mathcal{Z}(P))/c}, & \text{otherwise,} \end{cases} \tag{15}$$

where c is a control parameter having the interpretation of a *temperature* in annealing procedures. Thus, with a nonzero probability the computations will be continued with a configuration having a *larger* cost function compared to the previous configuration. The actual decision, whether or not P' should be accepted for $\mathcal{Z}(P') > \mathcal{Z}(P)$, is performed in the following way: P' is accepted, if

$$e^{-(\mathcal{Z}(P')-\mathcal{Z}(P))/c} \geq \eta, \tag{16}$$

where $\eta \in [0, 1]$ is a uniformly distributed random number. The value η is generated in each trial if $\mathcal{Z}(P') > \mathcal{Z}(P)$. Finally, the probability of performing the transition between P and P' is defined by

$$\mathbf{Pr}\{P \to P'\} = \begin{cases} G[P, P'] \cdot A[P, P'], & \text{if } P' \neq P, \\ 1 - \sum\limits_{Q \neq P} G[P, Q] \cdot A[P, Q]. \end{cases} \tag{17}$$

The probability $\mathbf{Pr}\{P \to P'\}$ depends on the control parameter c.

Let $\mathbf{a}_P(k)$ denote the probability of being in the configuration P after k steps performed for the same value of c. The probability $\mathbf{a}_P(k)$ can be calculated in accordance with

$$\mathbf{a}_P(k) := \sum_Q \mathbf{a}_Q(k-1) \cdot \mathbf{Pr}\{Q \to P\}. \tag{18}$$

The recursive application of (18) defines a Markov chain of probabilities $\mathbf{a}_P(k)$, where $P \in \mathscr{C}$ and $k = 1, 2, \ldots$. If the following conditions are satisfied for a given control parameter $c > 0$, for each $P \in \mathscr{C}_n$ the $\mathbf{a}_P(k)$ converges to the Boltzmann distribution $\mathbf{q}_c(P)$ (see [24, Eqs. (3.12), (3.14)]):

$$\begin{aligned} &\forall P_1, P_2\, \exists H_0, H_1, \ldots, H_s \in \mathscr{C}_n (H_0 = P_1 \& H_s = P_2): \\ &G[H_k, H_{k+1}](c) > 0, \quad k = 0, 1, \ldots, (s-1), \end{aligned} \tag{19}$$

and

$$\begin{aligned} &\forall c > 0\, \exists P_c, Q_c \in \mathscr{C}: \\ &A[P_c, Q_c] < 1 \wedge G[P_c, Q_c] > 0. \end{aligned} \tag{20}$$

Condition (19) provides the *irreducibility* of the Markov chain; condition (20) expresses the *aperiodicity* of $\mathbf{a}_P(k)$. If the generation and acceptance probabilities are defined as in (13) and (21), respectively, then conditions (19) and (20) are satisfied and one obtains the Boltzmann distribution as a result of $\mathbf{a}_P(k) \to \mathbf{q}_c(P)$ for $k = 0, 1, 2, \ldots$:

$$\mathbf{q}_c(P) = \frac{1}{F(c)} \cdot e^{-\mathcal{Z}(P)/c}, \tag{21}$$

where

$$F(c) = \sum_{P \in \mathscr{C}_n} e^{-\mathcal{Z}(P)/c} \tag{22}$$

is the partition function. That means, higher probabilities are assigned to configurations P with a lower cost function $\mathcal{Z}(P)$. For a changing control parameter c, i.e., if the "temperature" is lowered, one can prove the convergence property with respect to (13) and (15),

$$\lim_{c \to 0} \mathbf{q}_c(P) = \pi(P),$$

where

$$\pi(P) = \begin{cases} \left|\mathscr{C}_n^{\text{opt}}\right|^{-1} & \text{if } P \in \mathscr{C}_n^{\text{opt}}, \\ 0 & \text{elsewhere;} \end{cases}$$

see [24, Eqs. (3.4), (3.5)]. Thus, in contrast to deterministic methods (see, e.g., [5–7, 17, 20]), we do not exclude a priori the existence of several equilibrium states.

Because the computation of Markov chains, in general, is computationally intractable, one has to define some heuristic rules bounding the number L_c of transition steps for a fixed value of $c := c(t)$. Furthermore, it is necessary to determine how the parameter $c(t)$ has to be changed.

3.4. *Basic Parameters of Annealing Procedures*

For implementations of simulated annealing algorithms one has to define the concrete values or the computation rules for the following parameters:

1. Starting value $c(0)$, i.e., the initial "temperature;"
2. Length L_c of Markov chains for a fixed c;
3. Cooling schedule, i.e., how to lower the "temperature" after L_c changes of configurations have been performed (i.e., actual *changes*, not numbers of trials);
4. Stopping criterion $c(t_{\text{fin}})$, i.e., the final "temperature."

The value $c(0)$ has to provide that virtually all transitions $P \to P'$ are accepted; i.e., in accordance with (15), one has to ensure

$$e^{-\Delta\mathcal{Z}/c(0)} \approx 1. \tag{23}$$

While in general this condition cannot be verified efficiently, in our specific case of packing mixed rigid/nonrigid objects we can provide relatively tight bounds for $\Delta\mathcal{Z}$ and $c(0)$ which imply (23); see Section 4.1.

Once the parameter $c := c(t)$ has been chosen, the transitions between configurations are determined by (14) and (15). The process remains in configuration P until a differ-

ent configuration P' has been accepted. However, the computation of Markov processes is intractable due to the length of chains. For example, the lower bound

$$L_c \geq O(-\log \varepsilon) \cdot (|\mathscr{C}_n|^2 + 3 \cdot |\mathscr{C}_n| + 3)$$

is given in [24, Eq. (5.2)] with L_c being the number of computation steps necessary to approach an ε-distance to the stationary distribution $\mathbf{q}_c$, where one has to take into account that, in general, $|\mathscr{C}_n|$ grows exponentially in n (see (10) and (11)). There are numerous possibilities discussed in the literature dealing with the number L_c of steps actually performed for a fixed value of c. We will relate the number L_c to the following values:

1. The expected number $\widehat{R_c(P)}$ of trials that are necessary for leaving a given configuration P.
2. The neighbourhood cardinality $|\mathscr{N}_P|$.

An upper bound for $\widehat{R_c(P)}$ can be derived in the following way: By definition, the expectation $\widehat{R_c(P)}$ is expressed by

$$\widehat{R_c(P)} := \sum_{l=1}^{\infty} l \cdot \mathbf{Pr}\{\text{Leaving } P \text{ during the } l\text{th trial}\}.$$

The probability $\mathbf{Pr}\{\cdot\,\cdot\,\cdot\}$ is equal to the probability *not* to leave P during the first $(l-1)$ trials multiplied by the probability to leave P in the lth trial. Based on (17), one can show by straightforward calculations that

$$\widehat{R_c} \leq e^{\max_P \max_{P' \in \mathscr{N}_P} |\mathscr{H}(P') - \mathscr{H}(P)|/c(t)}$$

for arbitrary $P \in \mathscr{C}_n$. We set

$$\Delta\mathscr{H}_{\max} := \max_P \max_{P' \in \mathscr{N}_P} |\mathscr{H}(P') - \mathscr{H}(P)|.$$

Now, the two values considered for the actual length of Markov chains L_c are defined as

$$L_c^{(1)} := e^{\Delta\mathscr{H}_{\max}/c(t)} \geq \widehat{R_c}, \tag{24}$$

$$L^{(2)} := l \cdot (8 \cdot n + 1) = l \cdot (\max_{P \in \mathscr{C}_n} |\mathscr{N}_P|). \tag{25}$$

In the second equation the length does not depend on the temperature, and l is a small integer or a rational number $l < 1$ for large n and slow cooling schedules.

In order to perform a "slow cooling process," one should guarantee only small changes for c,

$$\frac{1}{1+\delta} < \frac{q_{c(t)}(P)}{q_{c(t+1)}(P)} < 1 + \delta \tag{26}$$

for a small real number δ. As shown in [2, Eqs. (4.8), (4.9)], both inequalities in (26) are satisfied if for all $P \in \mathscr{C}_n$:

$$c(t+1) > c(t) \Big/ \left[1 + \frac{\ln(1+\delta)}{\mathscr{H}_{c(t)}(P) - \mathscr{H}^{\text{opt}}} \cdot c(t)\right]. \tag{27}$$

This inequality can be taken as the basis for a decrementing rule, e.g., as described in Section 4.3. Another way is to take a simple decrementing rule like $c(t+1) := \alpha \cdot c(t)$ for a constant α smaller than but close to 1 (see Section 4.2).

The stopping criterion $c(t_{\text{fin}})$ can be derived, e.g., from the distance of the expected value of the cost function to the optimal value (see [2, Eq. (4.15)]), i.e., from $\Delta\widehat{\mathscr{H}_{c(t)}} := \widehat{\mathscr{H}_{c(t)}} - \mathscr{H}^{\text{opt}}$, where $\widehat{\mathscr{H}_{c(t)}} := \sum_P \mathscr{H}(P) \cdot \mathbf{q}_{c(t)}(P)$ is the expected cost value at $c(t)$. If we assume that $\widehat{\mathscr{H}_{c(t)}}$ is close to $\mathscr{H}^{\text{opt}}$ for low temperatures, the value $\Delta\widehat{\mathscr{H}_{c(t)}}$ can be approximated for small $c(t)$ by simply using the partial derivative,

$$\frac{\widehat{\mathscr{H}_{c(t)}} - \mathscr{H}^{\text{opt}}}{c(t) - 0} = \frac{\Delta\widehat{\mathscr{H}_{c(t)}}}{c(t)} \approx \frac{\partial\widehat{\mathscr{H}_{c(t)}}}{\partial c(t)}, \tag{28}$$

$$\Delta\widehat{\mathscr{H}_{c(t)}} \approx c(t) \cdot \frac{\partial\widehat{\mathscr{H}_{c(t)}}}{\partial c(t)}. \tag{29}$$

Let $\widehat{\mathscr{H}_{\max}}$ denote the expected cost function for large (infinite) values of $c(t)$. Based on (29), the algorithm can be terminated at step $t+1$ if

$$c(t) \cdot \frac{\partial\widehat{\mathscr{H}_c}}{\partial c}\Big|_{c=c(t)} \leq \varepsilon \cdot \widehat{\mathscr{H}_{\max}} \tag{30}$$

for a small positive number ε. That means, the change of the cost function $\Delta\widehat{\mathscr{H}_{c(t)}}$ is very small compared to the expected initial value of $\mathscr{H}$ at $c(0)$. For packing of mixed rigid and flexible objects one can calculate relatively tight approximations of $\partial\widehat{\mathscr{H}_{c(t)}}/\partial c$ (see Section 4.1).

In the case that $L := L_c$ is a constant and, therefore, *not* chosen related to $\widehat{R_c}$ (see Section 4.2), one can define $c(t_{\text{fin}})$ in the following way: The upper bound (24) depends on the actual temperature $c(t)$. Hence, if the expected number of trials necessary to leave a given configuration is larger than the actual value L for the length of Markov chains, it is indeed the time to finish the procedure of simulated annealing. That means, based on (24) one has in this case

$$L < e^{\Delta z_{\max}/c(t_{\text{fin}})}, \tag{31}$$

$$c(t_{\text{fin}}) < \frac{\Delta\mathscr{H}_{\max}}{\ln L}. \tag{32}$$

This choice of the final temperature is of interest, in particular, if $\Delta\mathscr{H}_{\max}$ can be approximated, as in our case of packing mixed rigid and flexible objects (see Section 4.1).

4. TWO ANNEALING HEURISTICS

We will employ the special structure of the underlying configuration space and the properties of the objective function in order to get tight bounds for the parameters of our annealing heuristics.

4.1. *Specification of Input Parameters*

Our annealing heuristics are designed not only for regular (hexagonal) initial packings, but for the general case of random initial placements. Thus, the initial placements from $\mathscr{C}_n$ are restricted only by the parameter $p_1 \geq \Delta_{\max}$, defining the maximum deformation for initial and intermediate arrangements during the computation of equilibrium packings (of course, $p_1 < d/2$).

The local forces $\mathbf{F}(u_j)$, including the direction α_j, $j = 1, ..., n$, and the objective function $\mathscr{Z}$ are computed as described in Section 3.2. In order to find an upper bound for local forces, we consider neighbouring disks acting on a central disk u_j within an angle of π, because for angles larger than π the forces would compensate each other at least in part. The maximum resultant vector sum in the perpendicular direction is achieved, if the force corresponding to the maximum deformation p_1 is acting continuously on the arc facing the angle π. We consider the case that two rigid materials are deformed, i.e., the forces calculated from (7) are doubled in order to determine the resultant force from the particular deformation (see Section 2.1). We denote

$$G(p_1) := \frac{2}{C_1 - C_2 \cdot (\alpha_1/2 + \sin(\alpha_1/2))} \cdot \frac{p_1}{s(p_1)}, \quad (33)$$

and recall that $G(p_1) \cdot l(u, v)$ represents the normalized force (see (7)). Here, α_1 is the fixed deformation angle corresponding to the maximum deformation p_1. We use the fact that for $ds = ds_\alpha = l(u, v)$ the value ds is related to an infinitesimal deformation angle $d\alpha$ by the equations

$$ds = 2 \cdot \frac{d}{2} \cdot \sin\frac{d\alpha}{2} = 2 \cdot \frac{d}{2} \cdot \frac{\sin(d\alpha/2)}{d\alpha/2} \cdot \frac{d\alpha}{2} = \frac{d}{2} \cdot d\alpha,$$

because $\lim_{x\to 0}((\sin x)/x) = 1$. Thus, if we assume that $G(p_1) \cdot ds$ is acting continuously on the arc between the angle 0 and π, we obtain

$$\begin{aligned}\int_0^\pi G(p_1) \cdot ds_\alpha &= \int_0^\pi G(p_1) \cdot \frac{d}{2} \sin\alpha \, d\alpha \\ &= \frac{d}{2} \cdot G(p_1) \cdot \int_0^\pi \sin\alpha \, d\alpha = \frac{d}{2} \cdot G(p_1) \cdot (-\cos\alpha \,|_0^\pi) \\ &= d \cdot G(p_1).\end{aligned}$$

Thus, the force can be calculated for infinitesimally small deformation triangles. Let $\mathscr{F}_{\max}(p_1)$ denote the maximum resultant force that "tries to move" a single unit in placements with p_1 as the maximum deformation depth.

LEMMA 1.

$$\mathscr{F}_{\max}(p_1) = \max_{1\leq j\leq n} |\mathbf{F}_j| \leq d \cdot G(p_1). \quad (34)$$

Now, the deformation angle in (33) is replaced in accordance with

$$\sin\frac{\alpha_1}{2} = 2 \cdot \sqrt{p_1/d - (p_1/d)^2},$$

and, therefore,

$$\frac{\alpha_1}{2} = \arcsin(2 \cdot \sqrt{p_1/d - (p_1/d)^2}).$$

Hence, for $S(p_1, d) := 2 \cdot \sqrt{p_1/d - (p_1/d)^2}$ and, based on (33), the upper bound from Lemma 1 can be expressed by

$$\mathbf{F}^{\max} := \frac{p_1 \cdot S^{-1}(p_1, d)}{C_1 - C_2 \cdot (\arcsin S(p_1, d) + S(p_1, d))}. \quad (35)$$

The value $\mathbf{F}^{\max}$ can be calculated directly from the input parameters of a given packing problem and is applicable to the criterion formulated in (30).

In a similar way we derive an upper bound for

$$\Delta\mathscr{Z}_{\max} := \max_{[P,P']\in\mathscr{N}} |\mathscr{Z}(P') - \mathscr{Z}(P)|, \quad (36)$$

which is an important parameter defining the run-time of simulated annealing procedures (see (23), (24), and (32)). Consider a disk u in a given position and the force $\mathbf{F}(u)$ assigned to u, i.e., "trying to move" u. This disk u is the only unit that is moved during the transition $P \to P'$. In order to simplify notations, we assume $\mathbf{F}_u$ to be oriented in the opposite direction of the move; otherwise it would be necessary to take the projection onto the move direction, but this projection is smaller than $|\mathbf{F}(u)|$. The maximum distance that u can be moved is $\sqrt{2} \cdot w$, along the grid diagonal. The maximum increase of the "moving" force will appear, if continuously the same maximum increase $\Delta F(u)[\sqrt{2} \cdot w]$ of the force is assumed within an angle from $-\pi/2$ to $+\pi/2$. This is a first component that enlarges $|\mathbf{F}(u)|$. Additionally, the "resistance" of disks from the opposite direction may decrease, but also only by a value calculated from $\Delta F(u)[\sqrt{2} \cdot w]$ for the entire angle π. Thus, given a deformation depth $\Delta \leq p_1 - \sqrt{2} \cdot w$, an

upper bound for the maximum increase (decrease) $\Delta F(u)$ $[\sqrt{2} \cdot w]$ related to d_α can be expressed by

$$\Delta F(u)[\sqrt{2} \cdot w] = G(\Delta + \sqrt{2} \cdot w) \cdot ds_\alpha - G(\Delta) \cdot ds_\alpha, \quad (37)$$

where G is calculated as in (33) for p_1. It was already mentioned in Section 2.2 that the second derivative of $G = G(\alpha)$ is positive for $\alpha \in (0, \pi)$. That means, the value $\Delta F_u(\sqrt{2} \cdot w)$ is upper bounded by $\Delta F(p_1) := (G(p_1) - G(p_1 - \sqrt{2} \cdot w)) \cdot ds_\alpha$. Let $\Delta \mathscr{F}_{\max}(p_1)$ denote the maximum change of a local force assigned to a single unit u that may occur during the transition $P \to P'$. If we again consider projections $\Delta F(p_1) \cdot \sin \alpha$ onto the direction of the move and apply the same calculations as for (34), we obtain

$$\Delta \mathscr{F}_{\max}(p_1) \leq 2 \cdot d \cdot (G(p_1) - G(p_1 - \sqrt{2} \cdot w)). \quad (38)$$

Up to now we have considered only the force assigned to the disk u that is moved during the transition $P \to P'$. But the objective function is the average value of all local forces. Although all disks, except u, remain unchanged in their position during $P \to P'$, the forces assigned to the units may change for units in contact with u in P and/or in P'. Let $m(p_1)$ denote the maximum number of disks that can be placed along the border of a single disk in placements restricted by the maximum deformation depth p_1. Since we are interested in an upper bound for $\Delta \mathscr{F}_{\max}(p_1)$, we consider the case that, during the move $P \to P'$, the force increases by $\Delta \mathscr{F}_{\max}(p_1)$ for $1 + m(p_1)/2$ disks (located in the opposite direction of $\mathbf{F}(u)$, including u). In the direction of $\mathbf{F}(u)$, the forces could decrease, but these changes are not taken into account for the upper bound (in a symmetrical case, the remaining difference would be $\Delta F(u)$). From the defining equations (12) and (38) we obtain, finally, an upper bound for the maximum difference of forces $\Delta \mathscr{F}_{\max}(p_1)$:

$$\Delta \mathbf{Z}^{\max}(p_1) := d \cdot \frac{m+2}{n} \cdot (G(p_1) - G(p_1 - \sqrt{2} \cdot w)). \quad (39)$$

Since our objective function represents the average force assigned to a single disk, the value $\mathbf{F}^{\max}$ is also an upper bound for $\mathscr{F}$. Thus, we obtain

LEMMA 2. *The following upper bounds are valid for arbitrary $P \in \mathscr{C}_n$ satisfying the restriction provided by the parameter p_1:*

$$\mathscr{F}_{\max}(P) \leq \mathbf{F}^{\max}(p_1); \quad (40)$$

$$\widehat{R_{c(t)}(P)} < e^{\Delta \mathbf{Z}^{\max}(p_1)/c(t)}. \quad (41)$$

The values $\mathbf{F}^{\max}$ and $\mathbf{Z}^{\max}$ can be calculated from (35) and (39), by using only input parameters of the given packing problem and an appropriate approximation of $m(p_1)$.

Finally, we analyze the convergence of annealing procedures computing equilibrium packings of mixed rigid and flexible objects, where we suppose $p_1 \leq d/2 - w$, because for this bound of deformation depth none of the combinations of placed disks is excluded; i.e., we ensure that any equilibrium packing can be approached. In order to show the convergence, we apply the sufficient conditions given in (19) and (20). For two configurations P_1 and P_2 one can define intermediate configurations H_k, $k = 0, 1, ..., s$, such that $H_0 = P_1$, $H_s = P_2$, and H_k, H_{k+1} differ only by the placement of a single unit. This is possible because we consider identical objects and the whole set $\mathscr{C}$ with, in fact, no restrictions on the deformation depth. As already mentioned in (14), the inequality $G[H_k, H_{k+1}] \geq 1/(8 \cdot n + 1) > 0$ is valid for all $k = 0, 1, ..., (s - 1)$. Thus, condition (19) is satisfied. If for a given $n < K$ and all pairs $[P, P'] \in \mathscr{N}$ it holds that $A[P, P'] = 1$ and $A[P', P] = 1$, then all placements represent the same value of $\mathscr{F}(P)$, i.e., the value $\mathscr{F}^{\text{opt}}$. Hence, we assume that the value of $n < K$ makes it possible to find two neighbouring placements P, P' such that $\mathscr{F}(P) \neq \mathscr{F}(P')$. Because $G[P, P'] \geq 1/(8 \cdot n + 1) > 0$ and, e.g., $A[P, P'] < 1$, the third condition (20) is also satisfied for numbers of elements $n \leq K - k_0$ that are not too close to K. Therefore, we have:

THEOREM 1. *The stochastic simulated annealing procedure minimizing $\mathscr{F}$ for placements of mixed rigid and flexible objects, which is based on (13) and (15), tends to the global minimum for $c \to 0$.*

Here we suppose virtually that stationary distributions of Markov chains are calculated for any $c(t)$. In practical applications, however, the computation of Markov processes is interrupted after a defined number of steps, bounded, e.g., by the number given in (41) or by $\max_P |\mathscr{N}_P|$.

4.2. *The First Cooling Schedule*

Based on (23) and (39), the starting value $c(0)$ is defined from

$$e^{-\Delta \mathbf{Z}^{\max}(p_1)/c(0)} = 1 - p_2, \quad (42)$$

$$c(0) = -\frac{\Delta \mathbf{Z}^{\max}(p_1)}{\ln(1 - p_2)}, \quad (43)$$

where p_2 is a small positive value and the second parameter of our approach.

The decrementing rule is given by the simple relation

$$c(t+1) := p_3 \cdot c(t), \quad (44)$$

where p_3 is close to but smaller than one. The stopping criterion is derived from

$$c(t_{\text{fin}}) \leq \frac{\Delta \mathscr{Z}_{\max}}{\ln[l \cdot (8 \cdot n + 1)]} \leq \frac{\Delta \mathbf{Z}^{\max}(p_1)}{\ln[l \cdot (8 \cdot n + 1)]}. \quad (45)$$

This criterion is motivated by the value of $\widehat{R_c}$ (see (32)), since for this value of $c(t_{\text{fin}})$ the expected number of trials necessary to leave P is larger than $L = l \cdot (8 \cdot n + 1)$, the number that is used for interrupting the computation of Markov chains for a fixed temperature $c(t)$.

Let $\widehat{\chi(c)}$ denote the *expected* ratio of the entire number of processed trials and L_c at temperature c. Since t_{fin} denotes the number of cooling steps, we can define the average value $\overline{\chi} := 1/t_{\text{fin}} \cdot \sum_c \widehat{\chi_c}$. Hence, the number of processed trials from $c(0)$ to $c(t_{\text{fin}})$ is for a constant length L of Markov chains given by $\overline{\chi} \cdot L \cdot t_{\text{fin}}$. Furthermore, let T_{loc} denote an upper bound for the time needed to perform

1. the calculation of local forces (see formula (7) and Section 3.2);
2. the updating of the objective function (also possible by local computations);
3. the local computations and decisions in accordance with (15) and (16); and
4. the updating of cooling parameters (if necessary in the actual step).

The calculation of local forces requires the information about surrounding units. The corresponding time is bounded by $O(m(p_1))$. The updating of the objective function can be performed by modifying only the forces for u and $S(u)$, where u denotes the moved disk. The disk u is chosen randomly, with direct access to the address containing the information about u. Hence, the time T_{loc} can be upper bounded by $O(m(p_1) \cdot (d \cdot \ln K)^{O(1)})$.

If the cooling schedule is chosen in accordance with (43), (44), and (45), the number of steps t_{fin}, reducing the parameter $c(t)$ can be calculated from

$$(p_3)^{t_{\text{fin}}} \cdot c(0) = c(t_{\text{fin}}),$$

or

$$(p_3)^{t_{\text{fin}}} \cdot \left(-\frac{\Delta \mathscr{Z}_{\max}}{\ln(1 - p_2)} \right) = \frac{\Delta \mathscr{Z}_{\max}}{\ln[l \cdot (8 \cdot n + 1)]}.$$

We obtain finally

$$t_{\text{fin}} \leq \left\lceil \frac{1}{\ln p_3} \cdot \ln \left(-\frac{\ln(1 - p_2)}{\ln[l \cdot (8 \cdot n + 1)]} \right) \right\rceil.$$

That means, the number of cooling steps does not depend on the objective function.

If the length of Markov chains is determined by L, the algorithm has to perform $L \cdot t_{\text{fin}}$ *accepted* moves before the algorithm halts because of (45).

THEOREM 2. *For $L := l \cdot (8 \cdot n + 1)$ and the first cooling schedule the expected run-time of computing near-equilibrium packings of n mixed rigid and flexible objects is upper bounded by*

$$T_I \lessapprox \frac{l \cdot (8 \cdot n + 1)}{\ln p_3} \cdot \ln \left(-\frac{\ln(1 - p_2)}{\ln[l \cdot (8 \cdot n + 1)]} \right) \cdot T_{\text{loc}} \cdot \overline{\chi}.$$

An upper bound for the number of grid nodes K is given in (11), and we can substitute $\ln K$ by $\ln n + d + O(1) = O(\ln n)$. Thus, if we assume $L = O(n)$ and a quadratic complexity for the basic arithmetic operations in local computations, i.e., $T_{\text{loc}} = O(\ln^2 K)$, we obtain an expected run-time bounded by $O(n \cdot \ln^2 n)$.

4.3. *The Second Cooling Schedule*

The initial temperature is chosen as defined in the first mode by Eq. (43). The control parameter $c(t)$ is decremented by the rule

$$c(t + 1) := \frac{c(t)}{1 + \varphi(\delta) \cdot c(t)}. \quad (46)$$

The function $\varphi(\delta)$ is derived from (27). The right side enlarges in (27), if $\mathscr{Z}^{\text{opt}}$ is omitted and $\mathscr{Z}_{c(t)}$ is replaced in our case by the upper bound $2 \cdot G(p_1)$. Hence, the function $\varphi(\delta)$ is defined by

$$\varphi(\delta) := \frac{\ln(1 + \delta)}{\mathbf{F}^{\max}(p_1)} < 1. \quad (47)$$

We employ (30) for the definition of $c(t_{\text{fin}})$. In our case, $\widehat{\mathscr{Z}_{\max}}$ can be upper bounded by

$$\lim_{c \to \infty} \widehat{\mathscr{Z}_c} = \widehat{\mathscr{Z}_{\max}} = \frac{1}{|\mathscr{C}_n|} \cdot \sum_P \mathscr{Z}(P) < \mathbf{F}^{\max}(p_1). \quad (48)$$

This follows directly from the definition of $\widehat{\mathscr{Z}_c} = \sum_P \mathscr{Z}(P) \cdot \mathbf{q}_c(P)$, the values of $\mathbf{q}_c$ for $c \to \infty$ (see (21) and (22)), and the upper bound (40). Furthermore, we make use of the approximation

$$\widehat{\mathscr{Z}_c} \lessapprox \frac{\ln |\mathscr{C}_n|}{c(0)} \cdot c^2 + c. \quad (49)$$

The approximation can be derived from the analysis of the entropy function $\mathscr{E}_c := -\sum_P \mathbf{q}_c(P) \cdot \ln \mathbf{q}_c(P)$. The value $\Delta \mathscr{Z}_c$ from (29) is in our case equal to $\widehat{\mathscr{Z}_c}$ because $\mathscr{Z}^{\text{opt}} = 0$ (for simplicity of notation we assume that equilibrium

packings are achieved on the grid structure $L \times H$; otherwise the objective function has to be changed to $\mathscr{Z}(P) - \mathscr{Z}_{\min}$, where $\mathscr{Z}_{\min}$ is the minimal value of the average force that can be achieved on the underlying grid). Thus, from (30), (48), (49)), and $\Delta\mathscr{Z}_c = \widehat{\mathscr{Z}}_c$ we obtain the condition

$$\frac{\ln|\mathscr{C}_n|}{c(0)} \cdot c^2 + c < \varepsilon \cdot \mathbf{F}^{\max}. \tag{50}$$

The value $\ln|\mathscr{C}_n|$ is replaced by the upper bound from (10):

$$\ln|\mathscr{C}_n| < n \cdot \ln K + n \cdot \ln\left(1 - \frac{n-1}{2} \cdot \mathbf{a}\right).$$

Here, the parameter $\mathbf{a}$ depends on the deformation depth p_1 (instead of $\Delta_{\max}$), and we use the notation

$$\mathbf{b} := n \cdot \left(\ln K + \ln\left(1 - \frac{n-1}{2} \cdot \mathbf{a}\right)\right). \tag{51}$$

Now, we obtain from (50) the stopping criterion

$$c(t) < \sqrt{c^2(0)/4 \cdot \mathbf{b}^2 + \varepsilon \cdot c(0)/\mathbf{b} \cdot \mathbf{F}^{\max}} - \frac{c(0)}{2 \cdot \mathbf{b}}. \tag{52}$$

Since $c(0)$, $\mathbf{F}^{\max}$, and $\mathbf{b}$ can be calculated from input coefficients of the given packing problem, the bound (52) can be directly used for parameter settings in annealing procedures.

Based on (30) and (46), we can derive an upper bound for the expected computation time. One can show by induction that (46) implies

$$c(t) = \frac{c(0)}{1 + t \cdot \varphi(\delta) \cdot c(0)} \quad \text{for } t = 0, 1, ... \tag{53}$$

If t_{fin} is defined as the value of t when (52) is satisfied for the first time, together with (53) one obtains

$$\begin{aligned} &\frac{c(0)}{1 + t_{\text{fin}} \cdot \varphi(\delta) \cdot c(0)} \\ &\quad < \frac{1}{2 \cdot \mathbf{b}} \cdot (\sqrt{c^2(0) + 4 \cdot \varepsilon \cdot c(0) \cdot \mathbf{b} \cdot \mathbf{F}^{\max}} - c(0)) \\ &\quad \leq \frac{c(0)}{1 + (t_{\text{fin}} - 1) \cdot \varphi(\delta) \cdot c(0)}. \end{aligned}$$

The second inequality is solved with respect to t_{fin}, and additionally, (43) and (47) are applied. Hence, one obtains the upper bound

$$t_{\text{fin}} \leq \sqrt{-\ln(1 - p_2) \cdot \mathbf{b} \cdot \mathbf{F}^{\max}/\varepsilon \cdot \Delta\mathbf{Z}^{\max} \cdot \ln^2(1 + \delta)}. \tag{54}$$

The upper bound is related to the approximation (49). Finally, we have:

THEOREM 3. *For a bounded length L of Markov chains and the second cooling mode the expected run-time of computing equilibrium placements for n mixed rigid and flexible objects can be upper bounded by*

$$T_{II} \lessapprox L \cdot \sqrt{\frac{-\ln(1 - p_2)}{\varepsilon \cdot \ln^2(1 + \delta)}} \cdot \sqrt{\frac{\mathbf{b} \cdot \mathbf{F}^{\max}}{\Delta\mathbf{Z}^{\max}}} \cdot T_{\text{loc}} \cdot \overline{\chi}.$$

The value $\mathbf{b}$ can be expressed by $\mathbf{b} = O(n \cdot \ln K)$ (see (51)). Thus, we obtain the time bound $T_{II} \lessapprox O(n \cdot \sqrt{n} \cdot \sqrt{\ln n} \cdot \ln^2 n) = O(n^{3/2} \cdot \ln^{5/2} n)$.

In the second cooling schedule the run-time is longer, compared to the bound given in Theorem 2, but one has a better control of the final outcome, because the objective function is explicitly used in this cooling schedule (see (52)). However, the first cooling schedule also provides packings with a relatively small local force for all disks.

The paper [3] deals with the problem why, indeed, relatively fast randomized algorithmic solutions computing packings close to equilibrium states can be expected for packings of flexible objects. The explanation is based on a polynomial upper bound for the number of cooling steps that are sufficient for ε-approximations of equilibrium states. In [3] we have shown that after n^a steps of an appropriate annealing procedure the probability to be in an equilibrium state is at least $1 - \varepsilon$, or in other words, $\sum_{H \notin \mathscr{C}_n^{\text{opt}}} \mathbf{a}_H(k) < \varepsilon$. The exponent a is defined by the inverse value w^{-1} of the grid step size, the diameter d (which is a multiple of w), and material constants, i.e., if these values are fixed, the exponent a is a constant and the number n increases as the placement area increases. Since in our definition *rigid* disks differ from *flexible* disks only by the order of magnitude of the material constants C_1 and C_2, the result on polynomial time convergence in distribution can be extended immediately to the case of mixed rigid and flexible objects.

5. SIMULATION RESULTS

Our approach is based on the assumption that equilibrium states of composite materials do not correspond to regular packings of circular shaped discs, i.e., that computations of relative displacements under external forces should start with equilibrium packings of deformed particles. Therefore, we suppose an initial deformation of disks within the regular hexagonal placement, which is taken as the starting configuration for computing a near-equilibrium packing without an external impact. The outcome, i.e., the near-equilibrium packing is then used as the initial placement for calculating relative displacements under external forces, where at both stages we suggest the application of stochastic simulations.

We have implemented both stochastic annealing procedures from Section 4.2 and Section 4.3, respectively, on a parallel 20-processor Sun SPARC2000. The parallel implementation is a straightforward adaptation of the sequential procedures. The rectangular placement area is subdivided in a regular way according to the number of available processors. The processors act asynchronously, and a particular unit is assigned to a certain processor depending on the actual position within the placement area, i.e., the assignment may change when a unit moves from one part of the subdivision to another.

With respect to the heuristics, described in Section 4, two modifications were introduced: An adaptive grid size and nonuniform distributions of the generation probabilities. In general, one can expect that in equilibrium states centers of disks are not located in grid nodes. In order to improve the final results calculated on the grid structure, an adaptive grid size was introduced which reduces the grid size during the final period of computation. We followed a simple procedure: One has to choose the starting grid size $w_{\max}$, the final grid size $w_{\min}$, the reduction step r, and a parameter σ which defines the final portion of the computation time, where the grid size is reduced. After $\lceil L \cdot (1 - \sigma) \cdot t_{\text{fin}} \rceil$ *accepted* steps of the annealing algorithm, the grid size will be lowered if

$$\left\lfloor L \cdot \sigma \cdot t_{\text{fin}} \cdot \frac{r}{w_{\max} - w_{\min} + 1} \right\rfloor$$

accepted moves have been performed. Furthermore, the generation probabilities are modified in the following way: For any of the n units, the direction α_{res} of $\mathbf{F}_{\text{res}}(u)$ is taken, and among the eight surrounding grid nodes of the center of a unit the node $k(\alpha_{\text{res}})$ located in the direction of α_{res} is chosen, according to a subdivision into sectors with an angle $\pi/4$. To placements P', representing the move to a grid node $k_j(\alpha_{\text{res}})$, $j = 1, 2, ..., n$, a higher probability is assigned,

$$G[P, P'] := \begin{cases} \dfrac{1-\rho}{n} & P' \triangleq k_j(\alpha_{\text{res}}); \\ \dfrac{\rho}{|\mathcal{N}_P| - n}, & \text{otherwise,} \end{cases}$$

where $j = 1, 2, ..., n$ and $\rho > 0$. Since $G[P, P'] > 0$ is still satisfied for any $P' \in \mathcal{N}_P$, the general convergence properties (see Theorem 1) remain unchanged.

The length of Markov chains was $10 \cdot (8 \cdot n + 1)$ for the first cooling schedule and $8 \cdot n + 1$ for the second cooling schedule. The initial grid width $w_{\max}$ in simulations of Section 5.2 and Section 5.3 was 10^{-4} mm, and we used $w_{\min} := 10^{-5} \cdot w_{\max}$; ρ was chosen equal to 0.3. All input parameters were calculated in accordance with (35), (39), and (43) for the "rigid" material. The maximum deformation depth p_1 depends on the number n of disks (see Section 5.1, ..., Section 5.3), but the remaining parameters are approximately the same, i.e., $p_2 \approx 0.1$ and $p_3 \approx 0.9$ for the first cooling schedule, and $\delta \approx 0.1$, $\varepsilon \approx 10^{-4}$ (see (50)) for the second cooling schedule.

TABLE II

Number of disks	325	500	1000	1500
Average number of disks per processor	16.25	25	50	75
First cooling schedule				
Run-time parallel (s)	1101	1153	2573	4057
Run-time serial (s)	16930	18491	45901	72451
Speedup	15.4	16.1	17.8	17.9
Second cooling schedule				
Run-time parallel (s)	26549	28068	113203	—

5.1. *General Performance Analysis*

First, we present the run-time analysis for serial and parallel computations. Since relatively large deformations p_1 and random initial placements have been chosen (in order to test the capability to compute near-equilibrium states for extreme cases), the material was restricted to only one elastic type (low-density polyethylenes, see Table I).

Table II shows the results from experiments on different numbers of placed objects. The diameter ranges from 0.5 mm (325 disks) to 0.1 mm (1500 disks). In all parallel experiments the number $\mathbf{p}$ of involved processors was equal to $\mathbf{p} = 20$. For the first cooling schedule with an expected serial run-time of $n \cdot \ln^2 n \cdot \overline{\chi}$ the parallel computation time is compared to single processor computations.

The difference of the speedup to the number of processors can be explained mainly by the amount of time that is needed for the memory management (by the operating system) and the handling of units assigned to more than a single subdivision. For the second cooling schedule serial computations were not performed for larger numbers of units due to the expected run-time of $n^{3/2} \cdot \ln^{5/2} n \cdot \overline{\chi}$.

The comparison of run-times has to take into account the average number $\overline{m}$ of units from the neighbourhood of the particular disk that is considered during a single transition $P \to P'$. The number $\overline{m}$ depends on p_1 (maximum deformation depth) and ranges in our case from 24 (325 disks) to 6 (1500 disks).

The example from Fig. 5 and Fig. 6 shows that indeed a regular, hexagonal-like packing is computed for the case of only a single material. The average residue force is relatively small, especially, if we compare it to the average force from the initial random placement.

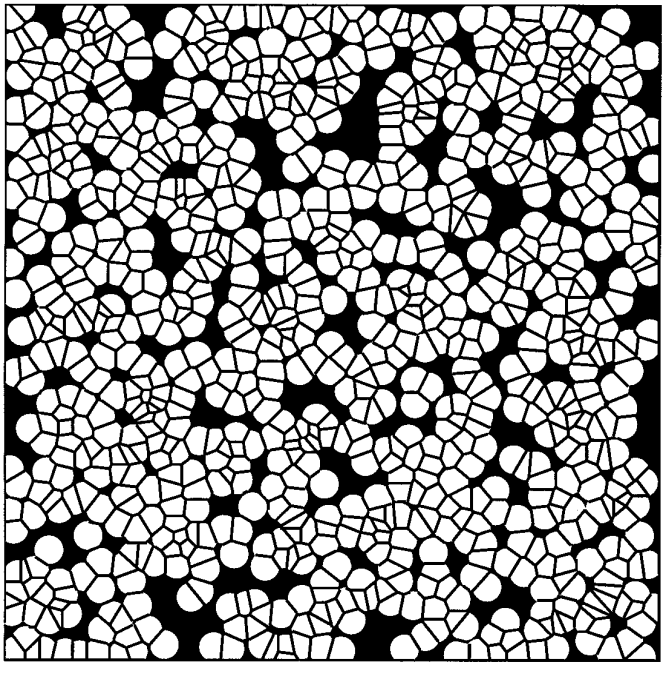

FIG. 5. Random initial placement: number of disks, 900 [900, 0]; diameter of disks, 0.15 mm; maximum deformation depth p_1, 0.06 mm; starting sum of forces, 1.24×10^4 *N*.

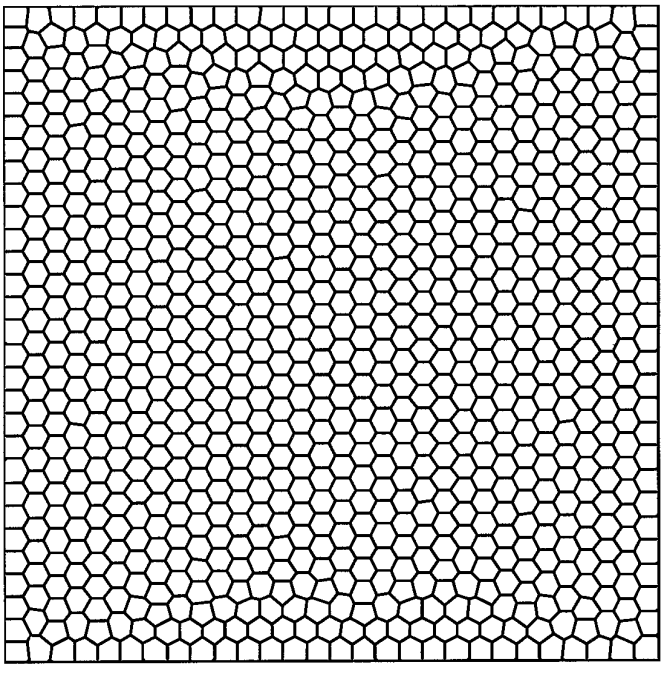

FIG. 6. Final packing: final sum of forces, 0.99 *N*; average residual force per disk, 0.0011 *N*; run-time (second schedule), 19 h 17 min 41 s ($\overline{\chi} \approx 1.1$).

5.2. *Relative Displacements to Regular Initial Packings*

Given two different materials, we consider the ratio $\kappa := |\mathbf{F}_I|/|\mathbf{F}_{II}|$ of forces that are necessary to achieve the same deformation depth Δ, where $|\mathbf{F}_I|$ and $|\mathbf{F}_{II}|$ are calculated from (7) and Δ is in a fixed, small relation to the diameter d. The force $|\mathbf{F}_I|$ corresponds to the *rigid* material. For example, if we take $\Delta/d = 1/100$ and the first two materials from Table I, we obtain $\kappa \approx 10^2$. As already mentioned in Section 1, the ratio of similar force constants is approximately 10^{12} in [20], and the ratio of rigid and nonrigid bond-stretching force constants is 10^7 in [17].

We consider simulation experiments mainly for two parameters: The force ratio κ and the maximum deformation depth $p_1 = \Delta_{\max}$. The constants $C^{el}_{1/2}$ of the "soft" material are taken from the first material of Table I, and we consider two values for κ: 10^2 and 10^5. The constants of the second ("rigid") material are simply from the division of $C^{el}_{1/2}$ by κ. The value $\kappa = 10^2$ does not correspond to our definition of rigid/nonrigid materials (see Section 2.2), but we try to

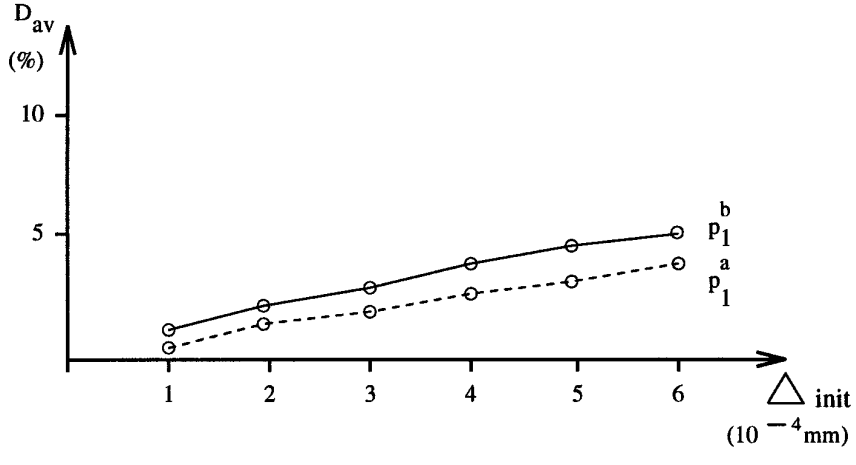

FIG. 7. Relative displacements: $\kappa = 10^2$.

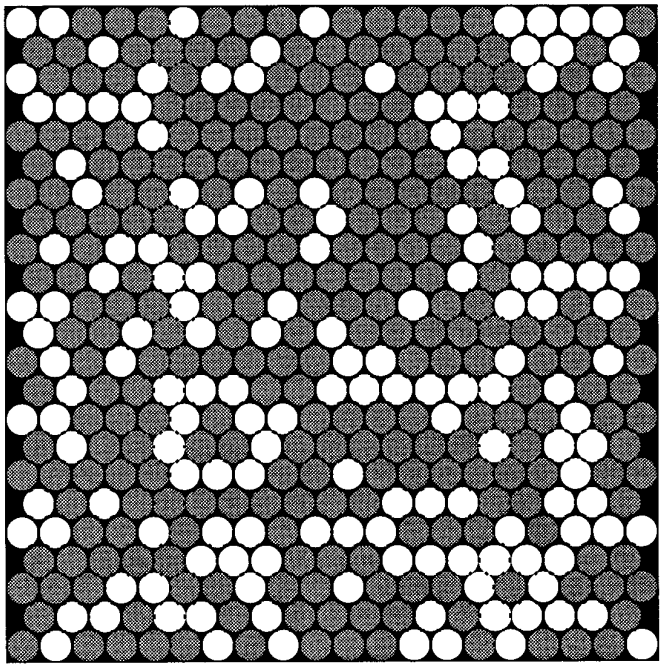

FIG. 8. Initial hexagonal packing: number of disks, 449 [156, 293]; initial deformation Δ_{init}, 0.0006 mm (d = 0.1602 mm); starting sum of forces, 2.88×10^5 N.

demonstrate that even in this case a measurable average displacement can be observed (Fig. 7).

By $[A, B]$ we denote A elastic disks and B rigid disks. Since we consider average displacements from hexagonal initial placements, the value of $B/(A + B)$ was chosen close to the percolation threshold $p_c = 1 - 2 \cdot \sin(\pi/18)$ of hexagonal networks (see [33]). Thus, for the case of 449 disks the corresponding number of "rigid" disks is 293 (or 294).

For an increasing diameter from 0.1592 mm up to 0.1602 mm we performed simulations with the first cooling schedule and two values of the parameter p_1: First, the maximum deformation p_1^a was taken 10 times larger than the deformation Δ_{init} of the initial regular placement, and, second, $p_1^b = 20 \cdot \Delta_{\text{init}}$ was chosen. In the initial hexagonal packing of Fig. 8, the deformation Δ_{init} is equal to 0.0006 mm, i.e., only ≈0.4% of the diameter 0.1602 mm. Except for the increasing diameter, all other settings are identical, and several runs were performed for a given diameter, but the outcome was nearly the same in all trials (see Fig. 8 and Fig. 9 for $\kappa = 10^2$ and $\Delta_{\text{init}} = 6 \times 10^{-4}$ mm).

As seen from Fig. 7, the average displacement D_{av} grows up to ≈5% of the radius even for $\kappa \approx 10^2$ and small values of Δ_{init}.

The simulations for $\kappa = 10^5$ were performed for the same range of the diameter and the same two values of $p_1^{a/b}$. We obtain $D_{\text{av}} \approx 9\%$ of the radius for $p_1^b = 0.012$ mm. The simulation results show that D_{av} increases only slightly if the maximum deformation depth changes from p_1^a to $p_1^b = 2 \cdot p_1^a$ (see Fig. 7 and Fig. 10).

5.3. *Relative Displacements under External Forces*

As a consequence of our simulations for small initial deformations and regular initial placements, we propose the following approach: First, by using the fast cooling schedule of Section 4.1, an equilibrium packing is calculated from a hexagonal initial placement. The average displacement is taken into account for the second step, where the impact of external forces is analyzed. The external force is simulated by lowering the upper boundary of the placement area. This corresponds to a permanent force, applied perpendicular to the upper boundary.

In Table III and Table IV we present the outcome of simulations for an initial deformation of 2×10^{-4} mm, i.e., ≈0.1% of the disk diameter 0.1028 mm. The constants $C_{1/2}^{el}$ are from the first material of Table I and κ was set to 10^5. The relation [371, 697] corresponds to the percolation threshold $p_c = 1 - 2 \cdot \sin(\pi/18)$.

The result from the first run of Table III was taken as the input for a second run, where a permanent external force was simulated by lowering the upper boundary. The height was decreased by 0.0002 mm, i.e., to disks u located

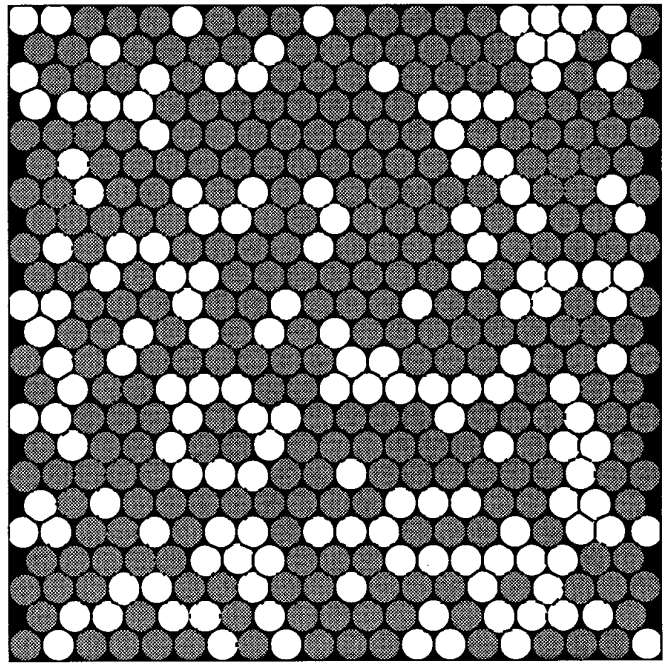

FIG. 9. Final packing: maximum allowable deformation p_1, 0.012 mm; maximum sum of forces, 3.26×10^5 N; final sum of forces, 3.06×10^2 N; (≈0.1% of max. force); average residual force per disk, 0.68 N; average displacement of disks, 0.0039 mm (≈5% radius); run-time (first schedule), 2 h 37 min 06 s, ($\overline{\chi} \approx 2.07$).

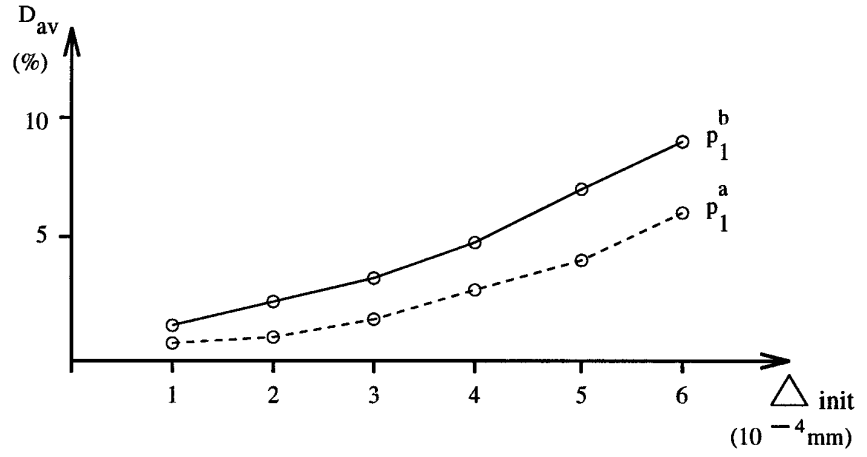

FIG. 10. Relative displacements: $\kappa = 10^5$.

at the upper boundary a force $\mathbf{F}(u)$ was assigned, where $|\mathbf{F}(u)|$ is calculated from (7) for $\Delta = 0.0002$ mm + displacement (depending on the actual position of u and to which material u belongs). The second run was performed by the parallel implementation of the second cooling schedule.

The starting force results from the average external force per disk (31 disks are placed in one row at the upper boundary) and the residual force of the first run. Since p_1 is relatively small, the value of $\overline{\chi}$ is significantly larger compared to Fig. 9, and this affects the run-time as already shown in Theorem 3.

6. CONCLUDING REMARKS

We have designed two stochastic procedures computing equilibrium packings of two-dimensional rigid and flexible objects. The algorithms are relatively independent of the particular physical modeling of interactions between objects; therefore, these heuristics can be applied to various physical problems, e.g., arising from the analysis of granular composites in material sciences. In the literature, two-dimensional granular composites are usually represented by networks of disks, where mainly two types of disks are considered, namely, deformable and rigid ones. While in existing approaches large systems of equations have to be solved in order to compute successive configurations, our algorithms are based on stochastic decisions about local changes in configurations. The general principle is derived from simulated annealing, and the expected run-time for the two types of cooling schedules can be upper bounded by $n^{3/2} \cdot \ln^{5/2} n$ and $n \cdot \ln^2 n$, respectively. In the first cooling schedule the run-time is longer, but because the objective function is explicitly used in the cooling schedule, one has a better control of the final outcome, resulting in placements with extremely small values of local forces for any unit; i.e., these placements are very close to equilibrium states. For both cooling schedules the expected run-time has indeed been achieved by our implementation, and the program runs relatively fast even for a large number of units. Although in the second cooling schedule the number of cooling steps does not depend on the objective function, our computational experiments have produced placements with a relatively small local force for any unit; i.e., these placements are also close to equilibrium states. The results from the parallel implementation show that even for a relatively large number of units the program runs very fast, and compared to the sequential case, the speedup is close to the maximum possible acceleration. Both heuristics were applied to stochastic simulations of composite packings, especially to computations of equilibrium packings from regular initial placements. Furthermore, we performed computational experiments where the impact of external forces is simulated by a decrease of the placement area. Relatively large average displacements of equilibrium packings from regular initial placements have been obtained, even for small initial deformations. For 449 disks and a ratio $\Delta_{\text{init}}/d \approx 0.004$ an average displacement of ≈5%

TABLE III

Number of disks	1068 [371, 697]
Diameter of disks	0.1028 mm
Initial deformation Δ_{init}	0.0001 mm
Max. allowable deformation p_1	0.001 mm
Maximum sum of forces	1.74×10^8 N
Final sum of forces	2.21×10^6 N
	(≈1.27% of max. force)
Average residual force per disk	2.07×10^3 N
Run-time (first schedule)	4 h 35 min 11 s ($\overline{\chi} \approx 1.82$)
Average displacement (first step)	0.0011 mm (≈2% radius)

TABLE IV

Number of disks	1068 [371, 697]
Diameter of disks	0.1028 mm
Max. allowable deformation p_1	0.005 mm
Starting sum of forces	7.14×10^6 N
Maximum sum of forces	1.56×10^8 N
Final sum of forces	8.51×10^5 N (≈0.54% of max. force)
Average residual force per disk	7.97×10^2 N
Run-time (second schedule)	37 h 10 min 13 s ($(\overline{\chi}) \approx 2.42$)
Force simulation depth	0.0002 mm
Average external force per disk	2.45×10^5 N
Total average displacement	0.0026 mm (≈5% radius)

of the disk radius has been calculated even for a small force constant ratio of 10^2. For 1068 disks an average displacement of ≈2% has been obtained, related to a force constant ratio of 10^5 and very small initial deformations. Future work will be concentrated on modeling the impact of external forces by specific boundary conditions and the implementation of the three-dimensional case.

ACKNOWLEDGMENTS

The authors thank the referees for their careful reading of the manuscript and helpful suggestions that resulted in an improved presentation. We are grateful to Ms. Leona Suet-ying Yuen for her expert drawing of the figures.

REFERENCES

1. E. H. L. Aarts and P. J. M. Laarhoven, Statistical cooling : A general approach to combinatorial optimization problems, *Philips J. Res.* **40,** 193 (1985).
2. E. H. L. Aarts and J. H. M. Korst, *Simulated Annealing and Boltzmann Machines: A Stochastic Approach* (Wiley, New York, 1989).
3. A. Albrecht, S. K. Cheung, K. S. Leung, and C. K. Wong, Provably fast simulated annealing algorithms computing equilibrium placements of flexible objects, manuscript.
4. C. Allain, J. C. Charmet, M. Clement, and L. Limat, Comparison of the elastic moduli and the conductivity observed in a two-dimensional percolating system, *Phys. Rev. B* **32,** 7552 (1985).
5. S. Arbabi and M. Sahimi, Mechanics of disordered solids. I. Percolation on elastic networks with central forces, *Phys. Rev. B* **47,** 695 (1993).
6. S. Arbabi and M. Sahimi, Mechanics of disordered solids. II. Percolation on elastic networks with bond-bending forces, *Phys. Rev. B* **47,** 703 (1993).
7. S. Arbabi and M. Sahimi, Mechanics of disordered solids. III. Fracture properties, *Phys. Rev. B* **47,** 713 (1993).
8. ASM International, *ASM Engineered Materials Reference Book* (ASM International Reference Publications, New York, 1989).
9. M. Babić, H. H. Shen, and H. T. Shen, The stress tensor in granular shear flows of uniform, deformable disks at high solids concentrations, *J. Fluid Mech.* **219,** 81 (1990).
10. R. J. Bathurst and L. Rothenburg, Micromechanical aspects of isotropic granular assemblies with linear contact interactions, *J. Appl. Mech.* **55,** 17 (1988).
11. D. J. Bergmann, Elastic moduli near percolation: Universal ratio and critical exponent, *Phys. Rev. B* **31,** 1696 (1985).
12. D. J. Bergmann, Elastic moduli near percolation in a two-dimensional random network of rigid and nonrigid bonds, *Phys. Rev. B* **33,** 2013 (1986).
13. D. J. Bergmann and E. Duering, Universal Poisson's ratio in a two-dimensional random network of rigid and nonrigid bonds, *Phys. Rev. B* **34,** 8199 (1986).
14. O. Catoni, Rates of convergence for sequential annealing: A large deviation approach, in *Simulated Annealing: Parallelization Techniques,* edited by S. Azencott (Wiley, New York, 1992), p. 25.
15. T. S. Chiang and Y. Chow, On the convergence rate of annealing processes, *SIAM J. Contr. and Opt.* **26,** 1455 (1988).
16. E. G. Coffman, Jr. and G. S. Lueker, *Probabilistic Analysis of Packing and Partitioning Algorithms* (Wiley, New York, 1991).
17. E. Duering and D. J. Bergman, Scaling properties of the elastic stiffness moduli of a random rigid-nonrigid network near the rigidity threshold: Theory and simulations, *Phys. Rev. B* **37,** 713 (1988).
18. G. Galambos and A. van Vliet, Lower bounds for 1-, 2- and 3-dimensional on-line bin-packing algorithms, *Computing* **52,** 281 (1994).
19. B. Hajek, Cooling schedules for optimal annealing, *Mathem. Oper. Res.* **13,** 311 (1988).
20. A. Jagota and G. W. Scherer, Viscosities and sintering rates of a two-dimensional granular composite, *J. Am. Ceram. Soc.* **76,** 3123 (1993).
21. W. S. Jodrey and E. M. Tory, Computer simulation of close random packing of equal spheres, *Phys. Rev. A* **32,** 2347 (1985).
22. V. B. Kashirin and E. V. Kozlov, New approach to the dense random packing of soft spheres, *J. Non-Cryst. Solids* **16,** 24 (1993).
23. S. Kirkpatrick, C. D. Gelatt, Jr. and M. P. Vecchi, Optimization by simulated annealing, *Science* **220,** 671 (1983).
24. P. J. M. Laarhoven and E. H. Aarts, *Simulated Annealing: Theory and Applications* (Reidel, Dordrecht, 1988).
25. L. Limat, Elastic and superelastic percolation networks: Imperfect duality, critical Poisson's ratios, and relations between microscopic models, *Phys. Rev. B* **40,** 9253 (1989).
26. N. Metropolis, A. W. Rosenbluth, M. N. Rosenbluth, A. H. Teller, and E. Teller, Equation of state calculations by fast computing machines, *J. Chem. Phys.* **21,** 1087 (1953).
27. D. Mitra, F. Romeo and A. Sangiovanni-Vincentelli, Convergence and finite-time behaviour of simulated annealing, *Adv. Appl. Prob.* **18,** 747 (1986).
28. F. Romeo and A. Sangiovanni-Vincentelli, A theoretical framework for simulated annealing, *Algorithmica* **6,** 302 (1991).
29. S. Roux and A. Hansen, Transfer-matrix study of the elastic properties of central-force percolation, *Europhys. Lett.* **6,** 301 (1988).
30. M. Sarrafzadeh and C. K. Wong, *An Introduction to VLSI Physical Design* (McGraw-Hill, New York, 1996).
31. M. Schulz and P. Reineker, Dilute and dense systems of random copolymers in the equilibrium state, *Phys. Rev. B* **53,** 12017 (1996).
32. C. Sechen and A. Sangiovanni-Vincentelli, The TimberWolf placement and routing package, *IEEE J. Solid-State Circ.* **20,** 510 (1985).
33. V. K. S. Shante and S. Kirkpatrick, An introduction to percolation theory, *Adv. Phys.* **20,** 325 (1971).
34. G. Sorkin, Efficient simulated annealing on fractal energy landscapes, *Algorithmica* **6,** 367 (1991).

35. I. M. Ward, *Mechanical Properties of Solid Polymers* (Wiley, New York, 1985).
36. D. F. Wong and C. L. Liu, Floorplan design of VLSI circuits, *Algorithmica* **4,** 263 (1989).
37. G. M. Zhang, Crossover exponents in percolating superconductor—Nonlinear-conductor mixtures, *Phys. Rev. B* **53,** 20 (1996).
38. A. Z. Zinchenko, An efficient algorithm for calculating multiparticle thermal interaction in a concentrated dispersion of spheres, *J. Comput. Phys.* **111,** 120 (1994).
39. A. Z. Zinchenko, Algorithms for random close packing of spheres with periodic boundary conditions, *J. Comput. Phys.* **114,** 298 (1994).